國立交通大學

機械工程學系

博士論文

重力平衡機構對機械手臂動態表現與壽命的影響評估

Evaluation of the Variation in Dynamic Performance and Service Life of a Manipulator after being Gravity Balanced

研 究 生　程貴仁
指導教授　鄭壁瑩 博士

中 華 民 國 100 年 7 月

重力平衡機構對機械手臂動態表現與壽命的影響評估

Evaluation of the Variation in Dynamic Performance and Service Life of a Manipulator after being Gravity Balanced

研 究 生：程貴仁　　Student：Cheng, Kuei-Jen

指導教授：鄭璧瑩 博士　　Advisor：Dr. Cheng, Pi-Ying

國立交通大學

機械工程學系

博士論文

A Dissertation

Submitted to Department of Mechanical Engineering

College of Engineering

National Chiao Tung University

in partial Fulfillment of the Requirements

for the Degree of

PhD

in

Mechanical Engineering

July 2011

Hsinchu, Taiwan, Republic of China

重力平衡機構對機械手臂動態表現與壽命的影響評估

研究生：程貴仁　　指導教授：鄭璧瑩 博士

國立交通大學機械工程學系

摘要

在工業界，機械手臂已被廣泛的應用在生產線上，以增進產能及降低成本。然而目前在工業界所常見的機械手臂有一共同的現象，即設計負載遠低於自重。此起因於機械手臂需具有相當剛性的結構，以避免因外加的負載而導致結構產生過大的應力變形而影響定位精度。然而機械手臂系統剛性的提升導致了自重的增加，自重的增加不但可能會降低該機械手臂動態的表現，也增加了機械手臂的能源消耗量。

機械手臂的動態表現常使用加速度半徑來表示。加速度半徑係用以度量一機械手臂在某特定組成及姿態下的動態表現，而該動態表現可藉由該機械手臂的組成、姿態及致動器的輸出能力來求得。當一機械手臂的動態表現是由加速度半徑代表時，其意指該機械手臂夾爪在該組成及姿態下，於所有方向可達成的最大加速度。

傳統上增進機械手臂動態表現的方法有下述兩種：1.增大所使用致動器的輸出；2.降低結構重量。然而增大所使用致動器的輸出意指需較多的能量輸入或（且）提升所使用致動器的輸出規格。輸出規格的提升往往導致較大的空間損耗與成本的投入或減少其減額比；而輸入較多能量不符合環保與成本節約的原則，且易導致減額比的下降而降低系統可能的壽命。

在降低結構重量部分，一般需使用更高級的材料、較複雜的結構形狀或減少系統剛性的方式達成。然而使用更高級的材料、較複雜的

結構形狀往往導致成本的增加；而減少系統剛性將使該機械手臂負載變形增加而降低其定位精度。故，傳統上所習用增進動態表現的兩種方式不但會導致較大的成本或空間損耗，且易使原機械手臂之可用性下降。

在大多數的應用上，致動器的輸出主要消耗在克服機械手臂原始重量，僅有少部分用以加速其所夾持的物件。有鑑於此，本研究探討當應用重力平衡原理–即使用外加機構來消除原機械手臂與外加機構的自重影響，增進能源使用效率與節省使用成本時可能產生的影響。由於外加機構能消雖除機械手臂的自重影響，但也改變了該機械手臂的原始構造，所以可能會影響該機械手臂的動態表現與壽命。為能解決此一問題，本研究利用操控性比來評估外加機構對機械手臂動態表現的影響，並利用加速度衰化率作為機械手臂動態表現受使用所產生的誤差而下降之評估標準，並進而評估該外加機構對原機械手臂的可能壽命之影響。

本研究所提出的方法，可有效的評估該應用重力平衡的外加機構對機械手臂動態表現與可能壽命的影響，使得設計人員得以同時評估機械手臂在能源使用效率、功能表現與可能使用壽命間的關係，以選出最佳符合該使用環境的機械手臂設計。

關鍵字：重力平衡；操控性比；加速度衰化率

Evaluation of the Variation in Dynamic Performance and Service Life of a Manipulator after being Gravity Balanced

Student：Cheng, Kuei-Jen　　Advisors：Dr. Cheng, Pi-Ying

Department of Mechanical Engineering
National Chiao Tung University

ABSTRACT

Manipulators have widely been utilized in industrial field to do assembly jobs in production lines. There are many different types of manipulators have been deployed for different applications, but most of them have a common characteristic, and that is the payload of a manipulator is much smaller than its self-weight. This is because a manipulator needs stiff structure to prevent from the excessive deformation resulted from the objects it holds to keep the positioning accuracy. However, the stiff structure results in the increase of the self-weigh and consumes considerable the output of the actuators of the manipulator. This not only increases the energy being consumed but also decreases the dynamic performance of the manipulator.

The dynamic performance of a manipulator is usually presented by acceleration radius. Acceleration radius is an index which is used to measure of the acceleration capacity of a manipulator with a certain configuration and at a specific posture. Dynamic performance will be influenced by the configuration, the posture, and the output capacity of the constituent joint actuators of the manipulator under discussion. When it is represented by acceleration radius, it means that the maximum acceleration which the end of a manipulator with certain configuration can achieve in all directions at that specific posture.

Conventionally, there are two approaches can be used to increase the dynamic performance of a manipulator, and they are: 1. raising the output

limits of the actuators it uses; 2. reducing the weight of the manipulator system. Raising the output limits of the actuators means that more energy needs to be exerted or/and the specification of the actuators needs to be promoted. However, raising the output limits of the actuators would result in cost increase, and exerting more energy will increase the cost and reduce the derating rate. Lowering derating rate usually results in the decline of the designed service life.

Reducing the weight of a manipulator system usually can be achieved by using better and stiffer materials or complicated but stiffer structures, or reducing the materials it uses. Using better materials and structure means the increase in the fabrication cost. Reducing the materials in use means the stiffness of the system decreases, and this will result in the deterioration in positioning accuracy which is caused by the increase of the compliance of the system. Based on what is stated above, these two conventional approaches used to promote the dynamic performance of a manipulator are not suitable to be implemented in real cases.

In most applications, the output of actuators of a manipulator spends on counterbalancing the gravitational force resulted from the stiff but heavy structure, not on accelerating the object it holds. To redeem this insufficiency, this study utilizes auxiliary mechanisms which is designed based on gravity balance theory to eliminate the influence of the self-weight of a manipulator and the mechanism. However, the auxiliary mechanism can eliminate the influence of self-weight but also changes the configuration of the original manipulator. This change may affect the dynamic performance and the service life of the manipulator. To cope with this issue, this study utilizes maneuverability ratio to evaluate the influence of an auxiliary mechanism on the dynamic performance of a manipulator after being equipped with that mechanism. Besides, this study also utilizes deterioration rate to investigate the deterioration in dynamic performance

of a manipulator with the errors resulted from the operation and evaluate the influence on the designed service life.

This study provides an effective methodology to evaluate the influence of a gravity balance mechanism on the dynamic performance and the designed service life of a manipulator. With the help of proposed methodology, designers of manipulators can not only have the ability to find out the relationship among the energy efficiency, performance, and designed service life of a manipulator but also have the capability to choose the best design to match the prescribed service conditions based on the results of evaluation.

Keywords: gravity balance; maneuverability ratio; acceleration radius

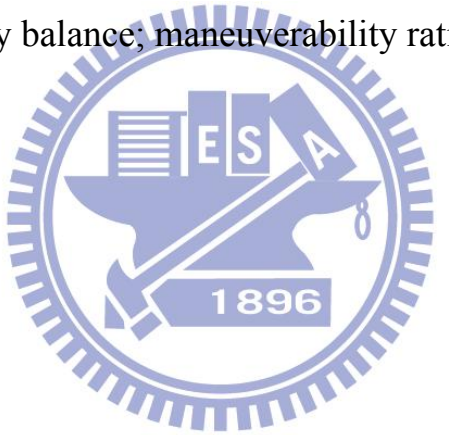

誌謝

感謝指導教授鄭璧瑩博士在這些年來的教導與協助，增進了學術研究相關的能力，並完成本論文。

感謝張起明博士與左明健博士在本論文寫作期間所提供的協助，也感謝口試委員金大仁教授、張起明博士、鍾添淦博士與陳昭亮博士對本論文的建議與指教。

感謝我的家人、親友在我求學期間所給予的支持與鼓勵，也感謝同師門的學弟們及所有給予我協助的人們。

感謝主，在您的關愛與許可下，學業得以完成。

感謝所有的一切。

程貴仁

2011年7月11日于新竹交大

Contents

List of Tables

Page

List of Figures

Page

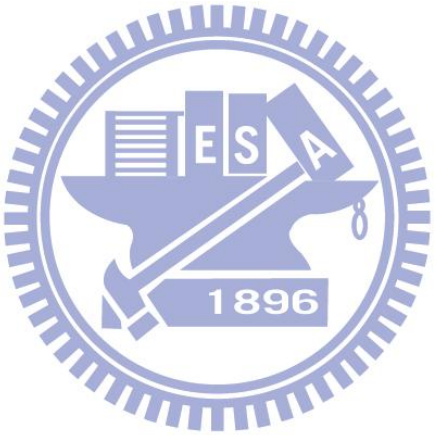

Glossary

m : Mass

c : Distance between the center of mass of a link and its corresponding joint

cm : Weight of counterweight

l : Length between two ends of a link or distance between two specified points of a link

wc : Distance between the center of mass of counterweight and its corresponding joint

r : Effective radius of a cam

k : Stiffness coefficient of a spring

g : Gravitational acceleration

θ : Angle between two specified objects around z axis (if applicable)

r_c : Actual radius of a cam

δ : Angle between effective and actual radiuses of a cam

f : External force

h : Vertical distance

s : Length associates with an auxiliary parallelogram

X : Position vector described in world space

r_i : Acceleration radius without the effect of errors

r_e : Acceleration radius with the effect of errors

d : Distance between two consecutive frames along z axis

α : Angle between two consecutive frames around x axis

a : Distance between two consecutive frames along x axis

A : D-H transformation matrix between two consecutive frames

T : D-H transformation matrix between two non-consecutive frames

R : Rotation part of D-H transformation matrix

P : Translation part of D-H transformation matrix

v : Linear velocity described in world space

w : Angular velocity described in world space

J : Jacobian matrix

q : Position vector described in the joint space

τ : Force or torque vector proposed by actuators

$c(q,\dot{q})$: Torque or force vector resulted from centrifugal and Coriolis forces

$g(q)$: Torque or force vector resulted from gravitational force

$M(q)$: Inertia matrix

L : Actuator output matrix

MR : Maneuverability ratio

β : Angle between two consecutive frames around y axis

H : Wear depth

S : Relative slide distance

K : Wear coefficient

p : Contact pressure

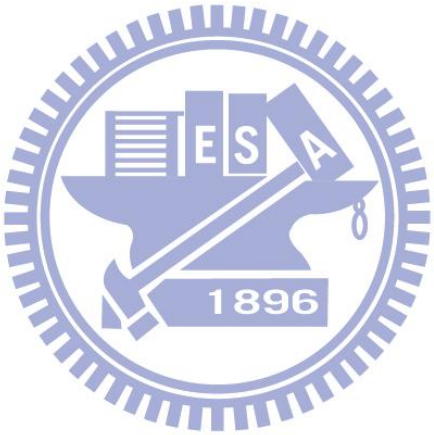

I. Introduction

This study investigates the variation in the dynamic performance and the designed service life of a manipulator after being equipped with a gravity balance mechanism. Service life means that a product can keep performing its designed functions without any unacceptable outcome. This study also proposes a methodology to evaluate the possible service life of a manipulator. Acceleration radius is usually utilized to be a measure of evaluating the dynamic performance of a manipulator with a certain configuration and at a specific posture, and it means that the maximum achievable acceleration in all directions at that posture. This study utilizes acceleration radius to evaluate the dynamic performance of a manipulator and uses maneuverability ratio to investigate and evaluate the variation in the dynamic performance of a manipulator before and after it is equipped with a gravity balance mechanism. Besides, deterioration rate is used in this study to evaluate the deterioration in dynamic performance of a manipulator resulted from the errors which are produced during the operation and to investigate how these errors influence the service life of a manipulator before and after being equipped with a gravity balance mechanism. In the following sections, the motivation and the goals of this study will be interpreted.

1.1 Motivation

In industrial field, many kinds of manipulators are designed to do the assembling job in the production line or perform some function in hazard environments. They indeed improve the productivity and quality of products and prevent humans getting injure from working environments. However, many of the manipulators used in industrial field have one common characteristic which is that the weight of the manipulator system itself is much greater than the payload at its end-effector. The stiff and

heavy structure is used to assure the stiffness of the manipulator is sufficient to counter the loading exerting on it to prevent excessive deformation which will deteriorate its positioning accuracy, especially when the manipulator is at a fully stretched posture. The stiff and heavy structure of a manipulator will consume considerable output energy of the constituent joint actuators to counterbalance the influence of self-weight even when this manipulator is in static working conditions. For many applications, manipulators spend most of their time on static or low-speed applications. However, these manipulators still need to spend considerable energy on counterbalancing their self-weight [1] even in these static or low-speed applications, and this will increase the operation cost.

To cope with this problem, the concept of gravity balance is proposed decades ago, and it successfully eliminates the influence of self-weight of a manipulator. For decades, gravity balance models and theories have been studied and investigated in a large volume of literature [2-22], such as the mathematical models of the auxiliary parallelogram approach [22]. In [5], it also emphasizes that after a manipulator has been gravity balanced, the energy efficiency of the manipulator shall become better, and the quantity of the energy can be saved by gravity balance mechanisms can be calculated by following the methodology provided in [1] and [10]. At the same time, many special designs have been developed and successfully satisfy the specific requirements of different applications [1, 23-31], such as an orthosis mechanism which can be used to assist the lower-limb disable patients to stand up from the sitting posture [33]. Meanwhile, the required actuator output which is used to perform a specific task before and after a manipulator is equipped with a gravity balance mechanism has been investigated in some studies [32]. However, as the author's best knowledge, there is no other researcher discusses what the variation in dynamic performance is before and after a manipulator is equipped with a gravity

balance mechanism, and they all focus on how to eliminate the influence of the self-weight or the required actuator output used to perform a specific task after a gravity balance mechanism is applied. Because manipulators are not just designed for or dedicated to static or low-speed applications and definitely not just designed for a specific task, this will lead to insufficient conclusions. How the gravity balance mechanism influences the dynamic performance after a manipulator is equipped with it needs to be considered.

After a gravity balance mechanism equips to a manipulator, the configuration of a manipulator is changed, and the loading exerting on each constituent joint and the mass arrangement of the system change too. This means the wear-out of each joint and dynamic performance of the manipulator will change associatively. Besides, the equipped gravity balance mechanism may make the dynamic performance of the manipulator more sensitive to the deviation of the parameters of Denavit–Hartenberg transformation matrix (D-H parameters) and may decline the designed service life which is based on the dynamic performance after the manipulator is equipped with a gravity balance mechanism. Although the subject of investigating the designed service life of a product has been studied for more than 50 years, there is limited literature which discusses the designed service life of a manipulator based on its functional performance, and all of the literature only takes the positioning [34-39] or velocity [36] performance as the functional performance of the corresponding manipulator. As the author's best knowledge, there is no other researcher discusses the designed service life of a manipulator including its dynamic performance which is represented by acceleration radius. This makes the study on the designed service life of manipulators insufficient.

Summarily speaking, the motivation of this study is to evaluate the

variation in the dynamic performance and the designed service life of a manipulator after being equipped with a gravity balance mechanism.

1.2 Literature Review

The concept of gravity balance was proposed decades ago, and its function is to counterbalance the self-weight of a manipulator to reduce the loading on the constituent joint actuators of a manipulator and promote the energy efficiency in static or low-speed applications. General speaking, there are two approaches can be used to satisfy the requirement of gravity balance. The first one is using counterweights to counterbalance the gravitational force resulted from the self-weight [5,8,18,23], and the other is utilizing springs and auxiliary links which include wires and cams to keep the summation of the gravitational potential energy of the manipulator system and the elastic potential energy of the spring system constant [1,4,12-15,17,19-20,22,24,27-29,31,33]. Although there are still other approaches which are able to keep manipulators in gravity balance [6,21,25-26,30], such as full spring approach [21], they are rarely used in practice.

In [5], [8], and [18], they investigate how to apply counterweights to the parallel mechanisms to eliminate the self-weight influence. In [23], it studies the torque which is needed to each joint actuator of a PUMA 760 robot arm to perform the motion which follows a prescribed trajectory after the robot arm is gravity balanced by using the counterweights.

How to use cams and springs to eliminate self-weight is introduced in [24] and [31]. Using auxiliary links and springs to form the orthosis to eliminate the self-weight influence is interpreted in [13-14], [17], [19], [28-29], and [33]. In [1], [4], [12], [15], [20], [22], and [27], using auxiliary links and springs to form auxiliary parallelograms to eliminate the self-weight is demonstrated.

[6] and [30] introduce how to only use auxiliary links to fix the center of mass of the whole system to a inertial position to keep the potential energy of this system invariant to achieve gravity balance. In [21] and [26], only using springs to fully or partially eliminate the self-weight influence is explained. Using strings to hang the weight of each links to eliminate the self-weight influence is introduced in [25].

In [2], it introduces how to use counterweights or auxiliary links and springs to eliminate the self-weight influence of planar linkages. [3] includes the effect of deformation into the discussion of a 2 DOF gravity balanced mechanism. In [7], it compares the influence of different transmission structures on the performance of gravity balance. [9] and [10] introduce how to use counterweights or auxiliary links and springs to eliminate the self-weight influence on certain postures or in a region. The performance comparison of a mechanism after being gravity balanced by counterweights and springs on lifting a certain weight is introduced in [11]. The classification of gravity balanced industrial robots is interpreted in [16]. In [32], it compares the velocity performance of a manipulator after being gravity balanced by counterweights and springs along a prescribed path.

Acceleration radius was proposed to be the index of measuring the dynamic performance of a manipulator with a certain configuration and at a specific posture in the 80's. In that period, the studying focus was on what the definition of dynamic performance would be and how to express it [40-42]. In the 90's, the dynamic performance of a redundant manipulator was wildly investigated, and these studies focused on finding the better expression and calculation methodology [43-48]. After the millennium, the influence of velocity on the dynamic performance of a manipulator started to be investigated [49-52]. Recently, the study on this field started to investigate the influence of the fabrication and assembly errors on the dynamic performance of a manipulator [53]. These studies really do a great

contribution on researching the dynamic performance of a manipulator and greatly progress the development in robotics.

The service life of a product started to be systematically investigated by the U.S. military in the 50's. For decades, much literature studied on this field had been proposed and promoted the quality of industrial products greatly. However, there are still few studies focus on the service life of a manipulator based on its functional performance until now [34-39]. All of these studies which investigate the service life of a manipulator only take the positioning or velocity performance as the functional performance of the manipulator, not including its dynamic performance.

1.3 Goal and Contribution

As the author's best knowledge, there is no other researcher investigates the variation in dynamic performance of a manipulator after being equipped a gravity balance mechanism, and this leads their conclusions on the applicability of gravity balance mechanisms insufficient. To rectify this insufficiency, this study utilizes acceleration radius as the index to evaluate the dynamic performance before and after a gravity balance mechanism equips to a manipulator. For gaining the quantitative information about how a gravity balance mechanism influences the dynamic performance of a manipulator, this study utilizes maneuverability ratio to evaluate whether being equipped with gravity balance mechanisms would improve or degrade the dynamic performance of a manipulator.

Because manipulators used in industrial field are not just for static or low-speed applications, the studying on the designed service life of manipulators should not be limited to the scopes of positioning accuracy and velocity performance as the functional performance. The evaluation of the designed service life of a manipulator should include its dynamic performance to match practical applications. To rectify this insufficiency,

this study utilizes deterioration rate as the dynamic performance deterioration index to evaluate the deterioration of dynamic performance of a manipulator and uses this index to investigate the variation in the designed service life which is based on the dynamic performance before and after the manipulation is equipped with a gravity balance mechanism.

This study not only discusses the variation in the dynamic performance of a manipulator before and after being equipped with a gravity balance mechanism, but also is the first one which discusses the designed service life of a manipulator based on its dynamic performance. The methodology proposed in this study includes using maneuverability ratio to evaluate the variation in dynamic performance and introducing the configuration errors into the model of acceleration radius to conduct deterioration rate to verify whether the dynamic performance is still acceptable after certain time in service. With the help of what is proposed by this study, the variation in the dynamic performance and the designed service life based on the dynamic performance of a manipulator after being equipped with a gravity balance mechanism can be found out. This can not only help designers of manipulators verify whether installing a gravity balance mechanism to a manipulator is beneficial to the application but also help them to choose the best design based on the requirements of the application.

In order to systematically and comprehensively introduce the fundamentals, methodology, and the conclusions used or proposed in this study, this study is arranged as follows: In Chapter II, it reviews the fundamentals of gravity balance, acceleration radius, maneuverability ratio, and deterioration rate. Chapter III interprets how to conduct maneuverability ratio to evaluate the variation in the dynamic performance of a manipulator before and after being equipped with a certain gravity balance mechanism. The designed service life evaluation of a manipulator

before and after being equipped with a certain gravity balance mechanism is performed in Chapter IV. Chapter V takes a PUMA 560 robot arm as an example to interpret how to use the proposed methodology and how it works. In Chapter VI, some conclusions are proposed.

II. Fundamental Review

In this chapter, it introduces the fundamental theories and approaches used in this study. For systematically introducing these theories and approaches, this chapter is arranged as follows: in Section 2.1, it introduces the fundamentals of each principle category of gravity balance mechanisms. How to conduct the acceleration radius to measure the dynamic performance of a manipulator with a certain configuration at a specific posture is explained in Section 2.2. Section 2.3 introduces how to conduct maneuverability ratio to evaluate the variation in the dynamic performance of a manipulator before and after being equipped with a gravity balance mechanism. In Section 2.4, how to conduct deterioration rate which is used to evaluate the influence of errors which is resulted from fabrication or assembly processes on the dynamic performance of a manipulator is provided.

2.1 Gravity Balance

Gravity balance means that using a special developed approach eliminates the influence of the self-weight of a manipulator or mechanism. Generally speaking, there are two approaches which can be applied to a manipulator or a mechanism to satisfy the definition of gravity balance without consuming any extra energy. The first one is the counterweight approach, and the other is the auxiliary link and spring approach. In the following subsections, the fundamental of each approach will be introduced.

2.1.1 The Counterweight Approach

The counterweight approach utilizes a counterweight to place the center of mass of a link and its successive links and their corresponding counterweights to the corresponding joint. The sequence of applying counterweights to a manipulator is from its last link to its first link

progressively. After applying a counterweight to the first link, the center of mass of the whole manipulator system locates at the joint which connects the base and the first link. Because the center of mass of the manipulator system is fixed to an inertial joint, the gravitational potential energy of the manipulator system will keep in constant from one posture to another. Since there is no change in the gravitational potential energy, it is no need to exert any force or work into the manipulator system to compensate the variation in its gravitational potential energy. For providing a clearer explanation of the concept and implementation of the counterweight approach, a two-link manipulator is taken as the example and shown in Figure 1. In the counterweight approach, the weight of each counterweight is unknown and needs to be calculated because it depends on the dimensions, configuration and weight arrangement of the manipulator. For this two-link example, the weights of each counterweight in use are shown in (1) and (2), respectively. For a general case, the weight of each counterweight can be calculated from (3) [33].

$$cm_1 = \frac{m_1 c_1 + (cm_2 + m_2) l_1}{wc_1} \tag{1}$$

$$cm_2 = \frac{m_2 c_2}{wc_2} \tag{2}$$

$$cm_i = \frac{m_i \cdot c_i + l_i \cdot \sum_{j=i+1}^{n} (cm_j + m_j)}{wc_i} \tag{3}$$

Where n is the number of links; cm_i and cm_j are the weight of counterweight of link i and link j respectively; m_i is the weight of link i; m_j is the weight of link j; c_i is the distance between the center of mass of link i and joint i; l_i is the length of link i; wc_i is the distance between the center of mass of the counterweight of

link i to joint i.

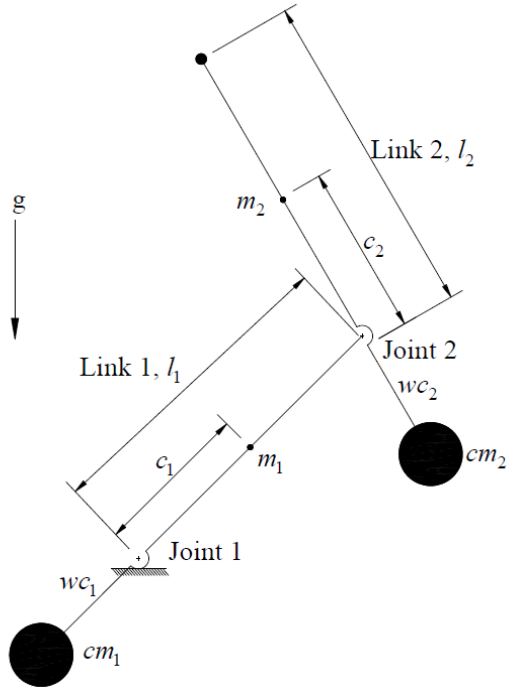

Figure 1: The counterweight approach – a two-link example

2.1.2 The Auxiliary Link and Spring Approach

In this approach, it utilizes springs to store or release the elastic potential energy to compensate the variation in the gravitational potential energy of a manipulator system. After appropriately adjusting and arranging the spring system, the sum of the gravitational potential energy of the manipulator system and the elastic potential energy of the spring system will be invariant when the manipulator moves from one posture to another. This means there is no need to exert any force or work into the manipulator system to compensate the variation in the gravitational potential energy when this manipulator moves from one posture to another. Generally speaking, the auxiliary link and spring approach includes three sub-approaches, and they are: the cam and the spring approach, the orthosis approach, and the auxiliary parallelogram approach. In the following subsections, the fundamental of each of the

three approaches will be introduced.

2.1.2.1 The Cam and Spring Approach

In the cam and spring approach, the contours of the cams are specialized according to the dimensions, configuration and weight arrangement of the manipulator they will be applied to. When in application, a spring will be dragged along with the contour of the corresponding cam to store or release its elastic potential energy to compensate the variation in gravitational potential energy of the corresponding link of the manipulator system. To explain this approach more clearly, a single link system is taken as the example and is shown in Figure 2. The contour of the cam of this example is depicted in Figure 3. When the diameter of the wire connecting the spring and the cam is negligible, the contour of the cam for this single link system can be conducted by following (4), (5), and (6) [24].

$$r = \sqrt{\frac{mgl}{2k}} \cdot (\sin\frac{\theta}{2} - \cos\frac{\theta}{2}) \tag{4}$$

$$r_c = \sqrt{\frac{mgl}{8k}(5 - 3\sin\theta)} \tag{5}$$

$$\delta = \tan^{-1}[-\frac{1}{2}(\csc\theta + \tan\theta)] \tag{6}$$

Where r is the effective radius of the cam; k is the stiffness coefficient of the spring; mg is the effective gravitational force of the self-weight; l is the distance from the joint axis to the location of the effective weight; θ is the angle between the link and the horizontal plane; c represents the real leave point of the wire to the cam; r_c is the actual radius following the cam shape; δ is the angle deviation between r and r_c.

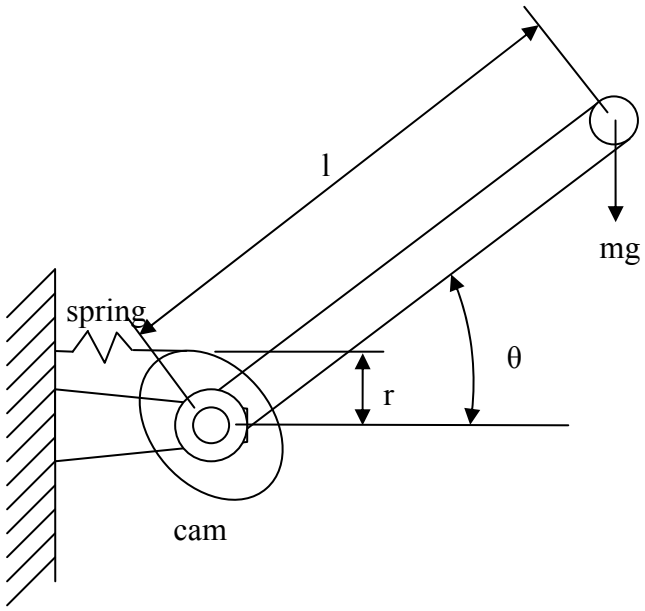

Figure 2: The cam and spring approach – a single link example

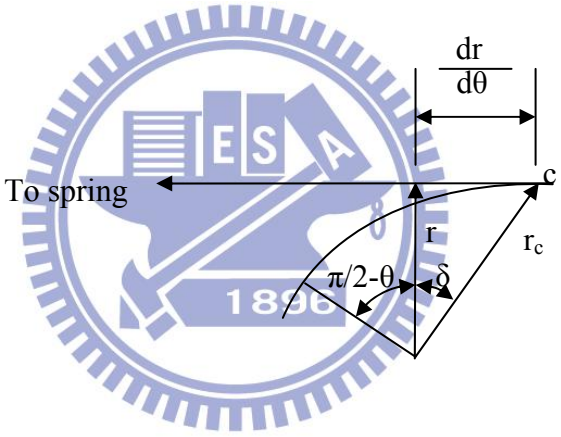

Figure 3: The contour of the cam

2.1.2.2 The Orthosis Approach

In the orthosis approach, it utilizes auxiliary links to create one or several parallelograms among the constituent links of a manipulator to identify or point to the center of mass of the manipulator system. Then a zero free length spring is used to connect the joint which identifies or points to the center of mass of the manipulator system to a certain inertial place. Then use other zero free length springs to connect each parallelogram to a certain place which depends on the dimensions, link number, configuration, and weight arrangement of the manipulator. In

this approach, the length of auxiliary link and the stiffness coefficient are the parameters need to be conducted. Figure 4 shows a two-link example which can be used to lift up heavy weight and external force in the gravitational direction with relative small input force, and the lengths of the auxiliary links ($l_1 - s_1$ and s_2) are expressed in (5) and (6) respectively, and the stiffness coefficients of the springs (k_1 and k_2) can be calculated by (7) and (8) respectively [33].

$$l_1 - s_1 = l_1 - \frac{s_2(m_1 g c_1 + m_2 g l_1 + f l_1)}{m_2 g c_2 + f l_2} \tag{5}$$

$0 < s_2 < l_2$, and s_2 must satisfy $0 < s_1 < l_1$ (6)

$$k_1 = \frac{s_1(m_2 g c_2 + f l_2)}{h s_2 (l_1 - s_1)} \tag{7}$$

$$k_2 = \frac{m_2 g c_2 + f l_2}{h s_2} \tag{8}$$

Where f is the external force exerted on the end point of link 2 in the gravitational direction; m_1 and m_2 are the masses of link 1 and link 2 respectively; c_1 and c_2 are the distance from the center of mass of link 1 to joint 1 and the distance from the center of mass of link 2 to joint 2 respectively; l_1 and l_2 are the lengths of link 1 and link 2 respectively; h is the vertical distance from one end of spring 2 to the base; θ_1 and θ_2 are the angles from the base to link 1 and the angle from link 1 to link 2 respectively.

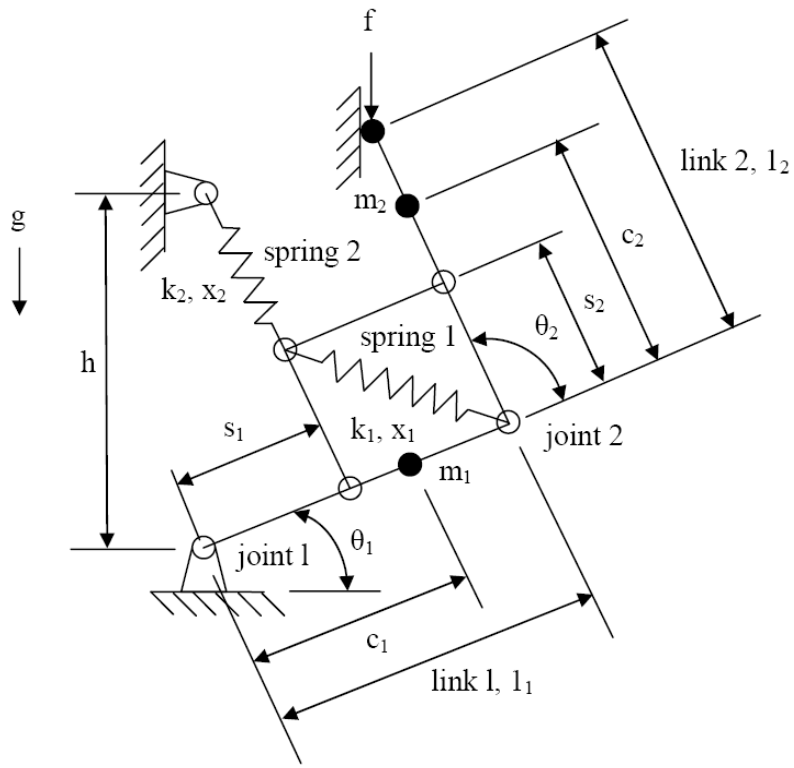

Figure 4: Two-link example of the orthosis approach

2.1.2.3 The Auxiliary Parallelogram Approach

Similar as the orthosis approach, the auxiliary parallelogram approach also uses auxiliary links to create one or more parallelograms. Differ from the orthosis one, these parallelograms are not used to find out or point to the center of mass of the manipulator system but create an environment which can make and treat each constituent link of the manipulator as an independent one. To explain this approach more clearly, a two-link manipulator is taken as the example and shown in Figure 5. In this approach, the masses of the auxiliary links may or may not be negligible. It depends on the weight of the auxiliary link and how the accuracy of the result it needs. If the weight of the auxiliary link is relative small when it compares with the one of the corresponding link of the manipulator or the required accuracy is not too high, the weight of the auxiliary link can be neglected to simplify

the calculation and evaluation. When the masses of the auxiliary links are negligible in this example, the stiffness coefficients of the springs can be expressed as (9) and (10), respectively. When the masses of the auxiliary links are not negligible, the general form of calculating the stiffness coefficient of each spring can be expressed as (11) [20].

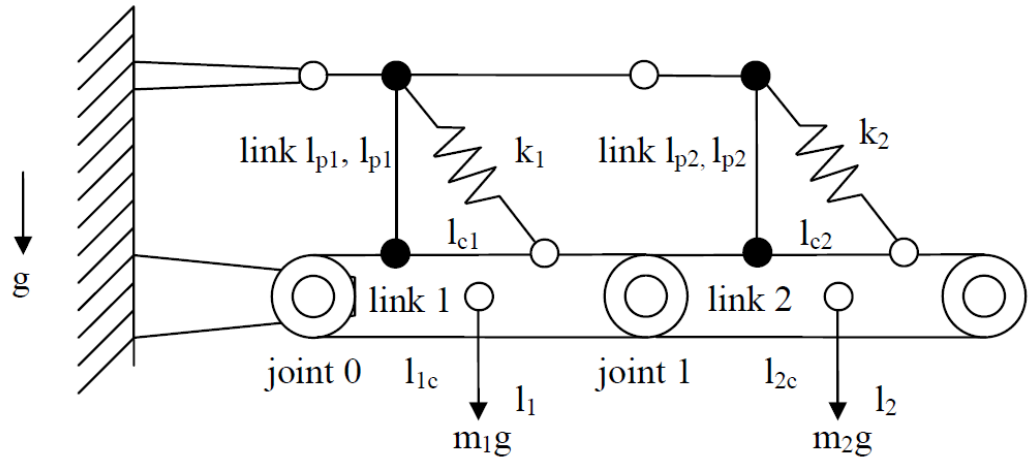

Figure 5: Two-link example of the parallelogram approach

$$k_1 = \frac{m_1 g \cdot l_{1c} + m_2 g \cdot l_1}{l_{c1} \cdot l_{p1}} \tag{9}$$

$$k_2 = \frac{m_2 g \cdot l_{2c}}{l_{c2} \cdot l_{p2}} \tag{10}$$

$$k_i = \frac{(m_i l_{ic} + \overline{m}_i \bar{l}_{ic} + \hat{m}_i \hat{l}_{ic}) \cdot g + \sum_{j=i+1}^{n} (m_j + \overline{m}_j + \hat{m}_j) l_i \cdot g}{l_{pi} \cdot l_{ci}} \tag{11}$$

Where k_i is the stiffness coefficient of the spring i; m_i and m_j are the masses of link i and link j respectively; $\overline{m}_i$ and $\overline{m}_j$ are the masses of auxiliary link i and auxiliary link j which are parallel to link i and link j respectively; $\hat{m}_i$ and $\hat{m}_j$ are the masses of auxiliary link i and auxiliary link j which are parallel to the gravitational direction respectively; l_{ic} is the distance between joint $i-1$ and the center of mass of link i; $\bar{l}_{ic}$ is the distance

along link i and between joint $i-1$ and the center of mass of auxiliary link i which is parallel to the gravitational direction; $\hat{l}_i$ is the distance from the joint which connects one end of auxiliary link i which is parallel to the gravitational direction and link i to joint $i-1$; l_{pi} is the height which is from the one end of spring i to the connecting joint of link l_{pi} and link i in the gravitational direction; l_{ci} is the distance which is along link i and between the one end of spring i to the connecting joint of link l_{pi} and link i.

2.2 Acceleration Radius

Acceleration radius is the index which is mostly used to measure the dynamic performance of a manipulator with a certain configuration at a specific posture under known output limits of the constituent joint actuators. Acceleration radius is defined as the maximum achievable acceleration in all directions of the end-effector of a manipulator at a specific posture. In Figure 6, it demonstrates a two degree of freedoms (DOF) example for providing a visual and clearer explanation of the definition of acceleration radius.

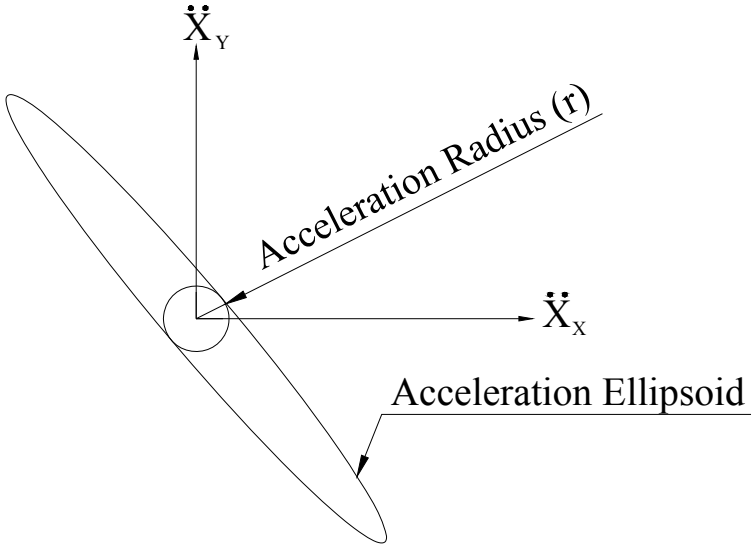

Figure 6: Definition of the acceleration radius with a 2 DOF example

Before introducing acceleration radius, Denavit-Hartenberg transformation matrix (D-H transformation matrix) must be interpreted first [54-55]. Conventionally, D-H transformation matrix is composed of 4 parameters to represent the transformation relationship between two consecutive links (frames or coordinates). These 4 parameters are: θ_i is the rotation angle between the two consecutive frames around z_i axis; d_i is the distance between the two consecutive frames along z_i axis; a_i is the distance between the two consecutive frames along x_i axis; α_i is the rotation angle between the two consecutive frames around x_i axis. In this study, these four parameters are called as D-H parameters. In Figure 7, it shows the diagrammatic definitions of these 4 parameters.

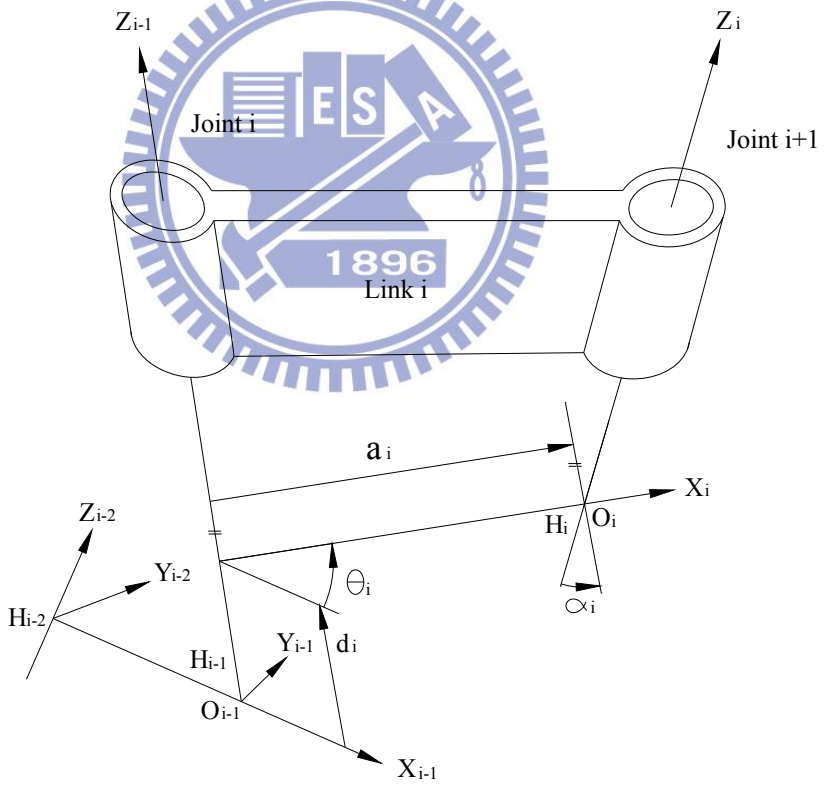

Figure 7. Diagrammatic definitions of D-H parameters

Based on the definitions of D-H parameters and their diagrammatic explanation shown in Figure 7, D-H transformation matrix from link i frame to link $i-1$ frame can be expressed as (12).

$$ {}^{i-1}A_i = \begin{bmatrix} C\theta_i & -S\theta_i C\alpha_i & S\theta_i S\alpha_i & a_i C\theta_i \\ S\theta_i & C\theta_i C\alpha_i & -C\theta_i S\alpha_i & a_i S\theta_i \\ 0 & S\alpha_i & C\alpha_i & d_i \\ 0 & 0 & 0 & 1 \end{bmatrix} \tag{12} $$

Where ${}^{i-1}A_i$ is the D-H transformation matrix from link i frame to link $i-1$ frame; S represents the sine function; C represents cosine function.

When a manipulator is composed of n links, the D-H transformation matrix from the frame which locates at the end-effector to the base or reference frame, T_n , can be expressed as (13).

$$ T_n = \prod_{i=1}^{n} {}^{i-1}A_i = \begin{bmatrix} R_n & P_n \\ 0 & 1 \end{bmatrix} \tag{13} $$

Where R_n is the rotation portion of T_n; P_n is the translate portion of T_n.

After introducing the total transformation matrix of a manipulator, how to conduct Jacobian matrix will be explained in the following discussion. Jacobian matrix is used to transform the constituent joint velocities of a manipulator in the joint space to the velocity of the end-effector in the world space. For a non-redundant manipulator, Jacobian matrix can be expressed as (14).

$$ \dot{x}_n = \begin{bmatrix} v_n \\ w_n \end{bmatrix} = J_{n\times n}\dot{q}_n \tag{14} $$

Where n is the number of the constituent joints; v_n is the linear velocity vector of the end-effector in the reference frame (world space); w_n is the angular velocity vector of the end-effector in the world space; $J_{n\times n}$ is the $n\times n$ Jacobian matrix; $\dot{q}_n$ is the constituent joint velocity vector in the joint space. v_n and w_n can be expressed as (15) and (16) respectively.

$$v_n = \sum_{i=1}^{n} \left[\dot{\theta}_i (z_{i-1} \times {}^{i-1}p_n) + z_{i-1}\dot{d}_i \right] \tag{15}$$

$$w_n = \sum_{i=1}^{n} \dot{\theta}_i z_{i-1} \tag{16}$$

Where z_{i-1} is the z axis direction of the $i-1$ frame which is described in the reference frame and equivalent to the 3rd column vector of R_{i-1}; ${}^{i-1}p_n$ is the position vector from end-effector to the origin of the $i-1$ frame and is also described in the reference frame; $\dot{\theta}_i$ is the angular velocity of the ith revolute joint; $\dot{d}_i$ is the linear velocity of the ith prismatic joint.

From (15) and (16), the general form of Jacobian matrix can be expressed as (17).

$$J = \left[J_1, J_2, ..., J_n \right] \tag{17}$$

Where $J_i = \begin{bmatrix} z_{i-1} \times {}^{i-1}p_n \\ z_{i-1} \end{bmatrix}$ is for a revolution joint, and $J_i = \begin{bmatrix} z_{i-1} \\ 0 \end{bmatrix}$ is for a prismatic joint.

After interpreting Jacobian matrix, the acceleration radius of a non-redundant manipulator will be introduced in the following. The first and second order differential kinematic equations of the end-effector of a non-redundant manipulator can be expressed as (18) and (19) respectively.

$$\dot{x}_n = J_{n\times n}(q)\dot{q}_n \tag{18}$$

$$\ddot{x}_n = \dot{J}_{n\times n}(q)\dot{q}_n + J_{n\times n}(q)\ddot{q}_n \tag{19}$$

Where q is the joint variable vector or angular position vector of the constituent joints described in the joint space; x is the position variable vector of the end-effector which is described in the reference frame.

The dynamic equation of a manipulator can be presented as (20).

$$\tau = M(q)\ddot{q} + c(q,\dot{q}) + g(q) \tag{20}$$

Where $\tau \in R^n$ is the vector of the constituent joint forces, torques, or both; $M(q) \in R^{n\times n}$ is the symmetric, positive definite inertial matrix; $c(q,\dot{q}) \in R^n$ is the vector of the forces, torques, or both resulted from centrifugal and Coriolis forces; $g(q) \in R^n$ is the vector of the force, torque, or both caused by external forces, torques, or both exerting on the manipulator.

From (20), the $\ddot{q}$ can be expressed as (21).

$$\ddot{q} = M^{-1}(\tau - c - g) \tag{21}$$

Take (21) into (19), $\ddot{x}$ can be expressed as (22).

$$\begin{aligned} \ddot{x} &= JM^{-1}(\tau - c - g) + \dot{J}\dot{q} \\ &= JM^{-1}\tau + (-JM^{-1}c + \dot{J}\dot{q}) + (-JM^{-1}g) \end{aligned} \tag{22}$$

Where $\ddot{x}$ is the acceleration vector of the end-effector which is described in the reference frame; $JM^{-1}\tau$ is the acceleration vector which is contributed by the constituent joint actuators; $(-JM^{-1}c + \dot{J}\dot{q})$ is the acceleration vector caused by the centrifugal and Coriolis forces; $(-JM^{-1}g)$ is the acceleration vector resulted from the gravitational force and external forces, torques, or both.

The output of an actuator used in industrial field usually has symmetric upper and lower limits. Thereof, the output range of each actuator used in a manipulator can be expressed as (23).

$$-\tau_i^{\text{limit}} \le \tau_i \le \tau_i^{\text{limit}} \quad , i = 1 \sim n \tag{23}$$

After normalizing (23), the normalized output vector of the constituent joint actuators, $\hat{\tau}$, can be expressed as (24).

$$\hat{\tau} = L^{-1}\tau \tag{24}$$

Where L is the diagonal matrix which the value of each diagonal

element is equal to the output limit of the corresponding actuator and can be expressed as (25).

$$L=\begin{bmatrix} \tau_1^{\text{limit}} & 0 & 0 \\ 0 & \ddots & 0 \\ 0 & 0 & \tau_n^{\text{limit}} \end{bmatrix} \tag{25}$$

Because $\hat{\tau}$ is a normalized matrix, it has the characteristic which can be expressed as (26).

$$\hat{\tau}^T\hat{\tau}\le 1 \tag{26}$$

Through (22) and (24), $\ddot{x}$ and $\ddot{\tau}$ can be expressed as (27) and (28) respectively after appropriate arrangement.

$$\ddot{x}=JM^{-1}L\hat{\tau}+(-JM^{-1}c+\dot{J}\dot{q})+(-JM^{-1}g) \tag{27}$$

$$\hat{\tau}=L^{-1}MJ^{-1}(\ddot{x}+JM^{-1}c-\dot{J}\dot{q}+JM^{-1}g) \tag{28}$$

Take (28) into (26), the equation of the acceleration ellipsoid can be conducted and expressed as (29).

$$(\ddot{x}+JM^{-1}c-\dot{J}\dot{q}+JM^{-1}g)^T J^{-T}M^T L^{-T}L^{-1}MJ^{-1}(\ddot{x}+JM^{-1}c-\dot{J}\dot{q}+JM^{-1}g)\le 1 \tag{29}$$

After taking $Q=J^{-T}M^TL^{-T}L^{-1}MJ^{-1}$ and substitute it into (29), a compact form of acceleration ellipsoid can be expressed as (30)

$$(\ddot{x}+JM^{-1}c-\dot{J}\dot{q}+JM^{-1}g)^T Q(\ddot{x}+JM^{-1}c-\dot{J}\dot{q}+JM^{-1}g)\le 1 \tag{30}$$

The value of acceleration radius is equal to the value of the radius of the smallest inner tangent sphere of the acceleration ellipsoid which is centered in the origin of the reference frame. When a manipulator is at a standing posture, the acceleration radius will be equal to the reciprocal of the square root of the maximum eigenvalue of Q.

2.3 Maneuverability Ratio

After a manipulator is equipped with a gravity balance mechanism, its configuration changes, and its dynamic performance may vary and would

not be the same as the original one. To evaluate this variation, maneuverability ratio is developed and used to evaluate the variation in dynamic performance of a manipulator before and after being equipped with a gravity balance mechanism or a mechanism used for other purposes. Maneuverability ratio at a specific posture can be defined as (31), and this ratio in a specific workspace can be expressed as (32). With the help of this ratio, it is easy to quantitatively evaluate how much the dynamic performance of a manipulator improves or deteriorates after being equipped with a gravity balance mechanism or a mechanism used for other purposes.

$$MR_P = \frac{r_g - r_o}{r_o} \tag{31}$$

Where MR_P is the maneuverability ratio at this specific posture; r_g and r_o are the acceleration radiuses after and before being equipped with a gravity balance mechanism respectively.

$$MR_W = \frac{\int_w (MR)dw}{\int_w dw} \tag{32}$$

Where MR_W is the maneuverability ratio in a prescribed workspace; $\int_w (MR)dw$ is the integral of the maneuverability ratio over the workspace; $\int_w dw$ presents the workspace; MR is the maneuverability ratio at dw; dw presents the differential area of the workspace.

If MR_P or MR_W is positive, this means that equipping with this gravity balance mechanism can improve the dynamic performance of the manipulator and eliminate the influence of self-weight. If MR_P or MR_W is negative, this means that being equipped with this gravity balance mechanism will sacrifice the dynamic performance of the manipulator though it eliminates the influence of self-weight. With the help of maneuverability ratio, designers of manipulators can get the information of how to adjust the setup of the controllers which will be used to perform the

trajectory planning automatically.

2.4 Deterioration Rate

Deterioration rate is an index of measuring the variation in the dynamic performance of a manipulator before and after including the influence of the errors which are resulted from the manufacturing, assembling, and operating processes. Deterioration rate is defined as the ratio of the deviation between the acceleration radius without and with the influence of the errors resulted from the manufacturing, assembling, and operating processes to the acceleration radius without these errors. The acceleration radius without the influence of these errors can be found out by using the processes provided in Section 2.2. However, finding out the acceleration radius with the influence of these errors which is due to the manufacturing, assembling, and operating processes is more complicated than finding the radius without the influence of these errors. How to conduct the acceleration radius with the influence of the errors resulted from the manufacturing, assembling, and operating processes will be explained in the following.

The first step of conducting the acceleration radius with the influence of the errors resulted from the manufacturing, assembling, and operating processes is to include the effect of these errors into the D-H parameters. The conventional D-H transformation matrix which has four D-H parameters is not sufficient to fully include the influence of these errors because it cannot include the angular error which is about the y axis. To cope with this insufficiency, an improved D-H transformation matrix which composes of five D-H parameters was proposed [56-58] and successfully includes all the effect of the errors resulted from the manufacturing, assembling, and operating processes into the transformation matrix. This kind of D-H transformation matrix which owns five D-H parameters is

called modified D-H transformation matrix hereafter. In the modified D-H transformation matrix, the extra parameter, β_i, is the rotation angle of the two consecutive frames about y_i axis and is shown in Figure 8. The modified D-H transformation matrix, ${}^{i-1}A_i^{'}$ can be conducted by post-multiplying the conventional D-H transformation matrix, ${}^{i-1}A_i$, with the rotation homogeneous matrix of β_i as shown in (33).

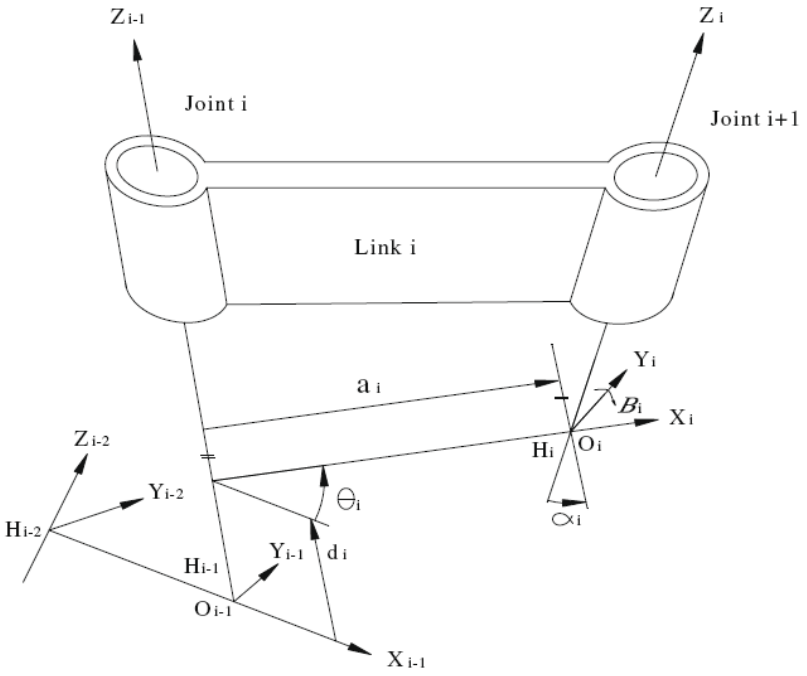

Figure 8: Diagrammatic definitions of modified D-H parameters

$$
\begin{aligned}
{}^{i-1}A_i^{'} &= {}^{i-1}A_i\, A(y_i,\beta_i) \\
&= \begin{bmatrix} C\theta_i & -S\theta_i C\alpha_i & S\theta_i S\alpha_i & a_i C\theta_i \\ S\theta_i & C\theta_i C\alpha_i & -C\theta_i S\alpha_i & a_i S\theta_i \\ 0 & S\alpha_i & C\alpha_i & d_i \\ 0 & 0 & 0 & 1 \end{bmatrix} \begin{bmatrix} C\beta_i & 0 & -S\beta_i & 0 \\ 0 & 1 & 0 & 0 \\ S\beta_i & 0 & C\beta_i & 0 \\ 0 & 0 & 0 & 1 \end{bmatrix} \\
&= \begin{bmatrix} C\theta_i C\beta_i - S\theta_i S\alpha_i S\beta_i & -S\theta_i C\alpha_i & C\theta_i S\beta_i + S\theta_i S\alpha_i C\beta_i & a_i C\theta_i \\ S\theta_i C\beta_i + C\theta_i S\alpha_i S\beta_i & C\theta_i C\alpha_i & S\theta_i S\beta_i - C\theta_i S\alpha_i C\beta_i & a_i S\theta_i \\ -C\alpha_i S\beta_i & S\alpha_i & C\alpha_i C\beta_i & d_i \\ 0 & 0 & 0 & 1 \end{bmatrix}
\end{aligned} \tag{33}
$$

Where $A(y_i,\beta_i)$ is the rotation homogeneous matrix of β_i. When β_i is equal to zero, (33) is fully equivalent to the conventional D-H transformation matrix as shown in (12). In fact, the purpose of existence of β_i is to include the rotation error about the y_i axis which is resulted from the manufacturing, assembling, and operating processes. Because β_i is used to introduce the influence of the angular error about the y_i axis, $\Delta\beta_i$, into the modified D-H transformation matrix, β_i itself has no intended function and is always assigned to be zero in practical applications. When the errors resulted from the manufacturing, assembling, and operating processes exist in the modified D-H parameters, the corrective modified D-H transformation matrix which includes the influence of these errors can be expressed as the sum of the original modified D-H transformation matrix and the differential change matrix. The corrective modified D-H transformation matrix can be expressed as (34).

$$^{i-1}A_i^C = {}^{i-1}A_i' + dA_i \tag{34}$$

Where $^{i-1}A_i^C$ is the corrective modified D-H transformation matrix; $^{i-1}A_i'$ is the modified D-H transformation matrix with nominal modified D-H parameters; dA_i is the differential change matrix resulted from the influence of the errors caused by the manufacturing, assembling, and operating processes. Because β_i is always zero, then $^{i-1}A_i' = {}^{i-1}A_i$, $C\beta_i = 1$, and $S\beta_i = 0$. To stress on the configuration errors have been introduced into the D-H transformation matrix, $^{i-1}A_i'$ will still be used in the following discussion. Assuming $\Delta\theta_i$, Δd_i, Δa_i, $\Delta\alpha_i$, and $\Delta\beta_i$ are the errors of θ_i, d_i, a_i, α_i, and β_i respectively. Because these errors are always much smaller than the corresponding nominal modified D-H parameters, dA_i can be presented as the linear combination of these errors

without significantly losing the representativeness, and it can be expressed as (35).

$$dA_i = \frac{\partial A_i}{\partial \theta_i}\Delta\theta_i + \frac{\partial A_i}{\partial d_i}\Delta d_i + \frac{\partial A_i}{\partial a_i}\Delta a_i + \frac{\partial A_i}{\partial \alpha_i}\Delta\alpha_i + \frac{\partial A_i}{\partial \beta_i}\Delta\beta_i \tag{35}$$

Set $\frac{\partial A_i}{\partial \theta_i} = D_\theta {}^{i-1}A_i$, $\frac{\partial A_i}{\partial d_i} = D_d {}^{i-1}A_i$, $\frac{\partial A_i}{\partial a_i} = D_a {}^{i-1}A_i$, $\frac{\partial A_i}{\partial \alpha_i} = D_\alpha {}^{i-1}A_i$, and $\frac{\partial A_i}{\partial \beta_i} = D_\beta {}^{i-1}A_i$.

Where $D_\theta = \begin{bmatrix} 0 & -1 & 0 & 0 \\ 1 & 0 & 0 & 0 \\ 0 & 0 & 0 & 0 \\ 0 & 0 & 0 & 0 \end{bmatrix}$; $D_d = \begin{bmatrix} 0 & 0 & 0 & 0 \\ 0 & 0 & 0 & 0 \\ 0 & 0 & 0 & 1 \\ 0 & 0 & 0 & 0 \end{bmatrix}$;

$D_a = \begin{bmatrix} 0 & 0 & S\theta_i & -d_i S\theta_i \\ 0 & 0 & -C\theta_i & d_i C\theta_i \\ -S\theta_i & C\theta_i & 0 & 0 \\ 0 & 0 & 0 & 0 \end{bmatrix}$; $D_\alpha = \begin{bmatrix} 0 & 0 & 0 & C\theta_i \\ 0 & 0 & 0 & S\theta_i \\ 0 & 0 & 0 & 0 \\ 0 & 0 & 0 & 0 \end{bmatrix}$;

$D_\beta = \begin{bmatrix} 0 & -S\alpha_i & C\theta_i C\alpha_i & a_i S\theta_i S\alpha_i - d_i C\theta_i C\alpha_i \\ S\alpha_i & 0 & S\theta_i C\alpha_i & -a_i C\theta_i S\alpha_i - d_i S\theta_i C\alpha_i \\ -C\theta_i C\alpha_i & -S\theta_i C\alpha_i & 0 & a_i C\alpha_i \\ 0 & 0 & 0 & 0 \end{bmatrix}$

From (35),

$$dA_i = (D_\theta \Delta\theta_i + D_d \Delta d_i + D_a \Delta a_i + D_\alpha \Delta\alpha_i + D_\beta \Delta\beta_i)^{i-1}A_i \tag{36}$$

Set $\delta^{i-1}A_i = D_\theta \Delta\theta_i + D_d \Delta d_i + D_a \Delta a_i + D_\alpha \Delta\alpha_i + D_\beta \Delta\beta_i$, then the corrective modified D-H transformation matrix can be expressed as (37).

$${}^{i-1}A_i^C = {}^{i-1}A_i' + d\,{}^{i-1}A_i = {}^{i-1}A_i' + (\delta^{i-1}A_i)\,{}^{i-1}A_i' \tag{37}$$

Where

$$\delta^{i-1}A_i$$

$$= \begin{bmatrix} 0 & -\Delta\theta_i & S\theta_i\Delta a_i & C\theta_i\Delta\alpha_i - d_iS\theta_i\Delta a_i \\ \Delta\theta_i & 0 & -C\theta_i\Delta a_i & S\theta_i\Delta\alpha_i + d_iC\theta_i\Delta a_i \\ -S\theta_i\Delta a_i & C\theta_i\Delta a_i & 0 & \Delta d_i \\ 0 & 0 & 0 & 0 \end{bmatrix}$$

$$+ \begin{bmatrix} 0 & -S\alpha_i\Delta\beta_i & C\theta_iC\alpha_i\Delta\beta_i & (a_iS\theta_iS\alpha_i - d_iC\theta_iC\alpha_i)\Delta\beta_i \\ S\alpha_i\Delta\beta_i & 0 & S\theta_iC\alpha_i\Delta\beta_i & (-a_iC\theta_iS\alpha_i - d_iS\theta_iC\alpha_i)\Delta\beta_i \\ -C\theta_iC\alpha_i\Delta\beta_i & -S\theta_iC\alpha_i\Delta\beta_i & 0 & a_iC\alpha_i\Delta\beta_i \\ 0 & 0 & 0 & 0 \end{bmatrix}$$

After conducting the corrected modified D-H transformation matrix, the total corrected modified D-H transformation matrix can be shown as (38).

$$T_n^C = \prod_{i=1}^{n} {}^{i-1}A_i^C = \prod_{i=1}^{n}(I + \delta^{i-1}A_i)^{i-1}A_i^{'} \tag{38}$$

Where n is the link number; I is a $n \times n$ identity matrix.

Because the kinematic deviation resulted from the error items, $\delta^{i-1}A_i$, is relatively small, the influence of the second and higher order terms can be omitted without any significant influence on the result. In the following discussion, only the first order approximation of (38) will be utilized, and it can be presented as (39).

$$T_n^C = T_n + \sum_{i=1}^{n} T_{i-1}\delta^{i-1}A_i\,{}^iT_n = (I + \sum_{i=1}^{n} T_{i-1}\delta^{i-1}A_iT_{i-1}^{-1})T_n$$

$$= \begin{bmatrix} R_n^C & P_n^C \\ 0 & 1 \end{bmatrix}$$

$$= \begin{bmatrix} R_n + (\sum_{i=1}^{n} R_{i-1}\delta r_iR_{i-1}^{-1})R_n & P_n + [\sum_{i=1}^{n}(R_{i-1}\delta r_iR_{i-1}^{-1})]P_n - \sum_{i=1}^{n}(R_{i-1}\delta r_iR_{i-1}^{-1}P_{i-1} - R_{i-1}\delta p_i) \\ 0 & 1 \end{bmatrix}$$

$$= \begin{bmatrix} [I + (\sum_{i=1}^{n} R_{i-1}\delta r_iR_{i-1}^{-1})]R_n & [I + \sum_{i=1}^{n}(R_{i-1}\delta r_iR_{i-1}^{-1})]P_n - \sum_{i=1}^{n}(R_{i-1}\delta r_iR_{i-1}^{-1}P_{i-1} - R_{i-1}\delta p_i) \\ 0 & 1 \end{bmatrix} \tag{39}$$

Where R_n^C is the rotation portion of T_n^C; P_n^C is the position portion of T_n^C; δr_i is the rotation part of $\delta^{i-1}A_i$; δp_i is the position part of $\delta^{i-1}A_i$.

When the corrected modified D-H transformation matrix and the total corrected modified D-H transformation matrix have been conducted, what should be done next is conducting the Jacobian matrix and acceleration ellipsoid which includes the influence of the errors which are resulted from the manufacturing, assembling, and operating processes. Because the process of conducting the Jacobian matrix and acceleration ellipsoid with the influence of the errors is similar with the one explained in Section 2.2, the following just shows and gives brief interpretations of some important concluded equations. The same as (14), v_n and w_n can be expressed as (40) and (41) respectively.

$$v_n = \sum_{i=1}^{n}\left[\dot{\theta}_i(z_{i-1}^C \times {}^{i-1}p_n^C) + z_{i-1}^C \dot{d}_i\right] \tag{40}$$

$$w_n = \sum_{i=1}^{n}\dot{\theta}_i z_{i-1}^C \tag{41}$$

Where z_{i-1}^C is the direction of z axis of the $i-1$ frame which is described in the reference frame and equivalent to the 3rd column vector of R_{i-1}^C, ${}^{i-1}p_n^C$ is the corrective position vector from end-effecter to the origin of the $i-1$ frame and is also described in the reference frame, $\dot{\theta}_i$ is the angular velocity value of the *ith* revolute joint, and $\dot{d}_i$ is the linear velocity value of the *ith* prismatic joint.

From the conduction shown in (39), z_{i-1}^C and ${}^{i-1}p_n^C$ can be presented as (42) and (43) respectively.

$$z_{i-1}^C = z_{i-1} + [(\sum_{j=1}^{i-1} R_{j-1}\delta r_j R_{j-1}^{-1})R_{i-1}]_z \tag{42}$$

$$
\begin{aligned}
{}^{i-1}P_n^C &= R_{i-1}[{}^{i-1}T_n]_P + R_{i-1}[d\,{}^{i-1}T_n]_P + dR_{i-1}[{}^{i-1}T_n]_P + dR_{i-1}[d\,{}^{i-1}T_n]_P \\
&= {}^{i-1}P_n + R_{i-1}[(\sum_{j=i}^{n} {}^{i-1}T_{j-1}\delta^{\,j-1}A_j\,{}^{i-1}T_{j-1}^{-1})\,{}^{i-1}T_n]_P + [(\sum_{j=1}^{i-1} R_{j-1}\delta r_j R_{j-1}^{-1})R_{i-1}][{}^{i-1}T_n]_P \\
&\quad + [(\sum_{j=1}^{i-1} R_{j-1}\delta r_j R_{j-1}^{-1})R_{i-1}][(\sum_{j=i}^{n} {}^{i-1}T_{j-1}\delta^{\,j-1}A_j\,{}^{i-1}T_{j-1}^{-1})\,{}^{i-1}T_n]_P
\end{aligned}
\tag{43}
$$

Where z_{i-1} is the direction of z axis of the $i-1$ frame presented in the reference frame which is equivalent to the 3rd column vector of R_{i-1}; ${}^{i-1}p_n$ is the position vector from end-effecter to the origin of the $i-1$ frame and also is described in the reference frame. The subscript "P" means the translation part of the bracketed transformation matrix and the subscript "Z" means the direction of z axis of the bracketed rotation matrix equivalent to the 3rd column vector.

From (40) and (41), the corrective Jacobian matrix can be expressed as (44).

$$
J^C = \left[J_1^C,\ J_2^C, \ldots, J_n^C \right] \tag{44}
$$

Where $J_i^C = \begin{bmatrix} z_{i-1}^C \times {}^{i-1}p_n^C \\ z_{i-1}^C \end{bmatrix}$ is for a revolution joint, and $J_i^C = \begin{bmatrix} z_{i-1}^C \\ 0 \end{bmatrix}$ is for a prismatic joint.

Substitute (42) and (43) into (44) and eliminate the second order term, J_i^C can be presented as (45).

$$
J_i^C = J_i + dJ_i \tag{45}
$$

Where J_i is the *ith* column of the nominal Jacobian matrix without the influence of the errors resulted from the manufacturing, assembling, and operating processes, and dJ_i is the differential change Jacobian matrix resulted from the influence of these errors.

In (46) and (47), they show J_i and the first order dJ_i of a revolute joint respectively.

$$J_i = \begin{bmatrix} z_{i-1} \times {}^{i-1}p_n \\ z_{i-1} \end{bmatrix} \tag{46}$$

$$dJ_i = \begin{bmatrix} z_{i-1} \times P_e + z_{de} \times {}^{i-1}P_n \\ z_{de} \end{bmatrix} \tag{47}$$

Similarly, in (48) and (49), they represent J_i and dJ_i of a prismatic joint, respectively.

$$J_i = \begin{bmatrix} z_{i-1} \\ 0 \end{bmatrix} \tag{48}$$

$$dJ_i = \begin{bmatrix} z_{de} \\ 0 \end{bmatrix} \tag{49}$$

Where $z_{de} = [(\sum_{j=1}^{i-1} R_{j-1}\delta r_j R_{j-1}^{-1})R_{i-1}]_z$ is the error in the direction of z axis of the $i-1$ frame, and $P_e = R_{i-1}[(\sum_{j=i}^{n} {}^{i-1}T_{j-1}\delta^{j-1}A_j {}^{i-1}T_{j-1}^{-1})^{i-1}T_n]_P + [(\sum_{j=1}^{i-1} R_{j-1}\delta r_j R_{j-1}^{-1})R_{i-1}][{}^{i-1}T_n]_P + [(\sum_{j=1}^{i-1} R_{j-1}\delta r_j R_{j-1}^{-1})R_{i-1}][(\sum_{j=i}^{n} {}^{i-1}T_{j-1}\delta^{j-1}A_j {}^{i-1}T_{j-1}^{-1})^{i-1}T_n]_P$ is the position error resulted from the influence of the configuration errors which are from the end-effecter to the $i-1$ link.

When the D-H transformation matrix and Jacobian matrix with and without the effect of the errors caused by the manufacturing, assembling, and operating processes are known, the acceleration radius with and without the effect of these errors can be conducted through the method proposed in Section 2.2. When the acceleration radiuses with and without the effect of these errors are known, deterioration rate can be defined as (50) [53].

$$DR_P = \frac{r_i - r_e}{r_i} \tag{50}$$

Where DR_P is the deterioration rate of a manipulator with a certain

configuration at a specific posture; r_e and r_i are the acceleration radius of a manipulator with a certain configuration at a specific posture with and without the influence of the errors resulted from the manufacturing, assembling, and operating processes respectively.

For a certain workspace or region, the deterioration rate over this workspace or region can be defined as (51), and it can be taken as a representative index of derating margin of the manipulation over this workspace or region [53].

$$DR_W = \frac{\int_w (dr) dw}{\int_w dw} \tag{51}$$

Where DR_W is the deterioration rate over a prescribed workspace or region, $\int_w (dr) dw$ is the integral of the deterioration rate which is over this workspace or region , $\int_w dw$ presents the workspace or region in discussion, dr is the differential function of deterioration rate, and dw presents the differential area of the workspace or region.

With the help of deterioration rate, designers of manipulators can estimate the degradation on the dynamic performance of a manipulator which is caused by configuration errors and handle the specification of the dynamic performance of a manipulator more correctly.

III. Evaluate the Variation in Dynamic Performance of a Manipulator after being Equipped with a Gravity Balance Mechanism

Using cams and springs to achieve gravity balance of a manipulator is feasible but not practical because accurately fabricating the contours of the cams is usually very difficult due to the requirements on highly non-linear contour surface. Besides, a rope or wire would not fully be along with the contour of a cam in most of occasions because of its stiffness. Applying the orthosis approach to a manipulator to reach gravity balance is feasible and practical, but its application is usually limited on a manipulator with less constituent links. This is because in the orthosis approach, the arrangement of the spring system highly depends on the dimensions, configuration and weight arrangement of the manipulator which it would be applied, and it is not easy to find a feasible one when the link number is more than two. Besides this, in the orthosis approach, the interference usually occurs between the auxiliary links, spring and the objects which locate inside the region of the workspace because of the complicated layout.

For the majority of manipulators used in industrial field, they usually have three or more links to assure that they can reach any point in their three dimensional workspace. Therefore, only the counterweight and auxiliary parallelogram approaches are practical and suitable to be applied to a manipulator used in industrial field to eliminate the influence of the self-weight of a manipulator.

Based on the reasons stated above, this study will only discuss how a gravity balance mechanism based on the counterweight or auxiliary parallelogram approach influences the dynamic performance of a manipulator after being equipped with it. In the following sections, they will explain how to conduct the dynamic performance of a manipulator after it is equipped with a gravity balance mechanism based on each of these two approaches.

3.1 The Dynamic Performance of a Manipulator after being Equipped with a Gravity Balance Mechanism Based on Counterweight Approach

When a manipulator uses the counterweight approach to achieve gravity balance, a counterweight needs to be applied to each link to eliminate the influence of the self-weight of this link and its successive links with their corresponding counterweights. This will result in the increase of the mass and moment of inertia of each link and the manipulator system. However, the applied counterweights can also eliminate the influence of the self-weight of each constituent link of the manipulator system. For this approach, the mass of the counterweight of each link can be conducted by (3), $cm_i = \dfrac{m_i \cdot c_i + l_i \cdot \sum_{j=i+1}^{n} (cm_j + m_j)}{wc_i}$. If the counterweight of link i can be taken as a point mass, the moment of inertia of this link with its corresponding counterweight to joint i, can be expressed as (52) where the effect of the successive links is excluded.

$$I_{GBCL_i} = I_i + (1 + \frac{m_i}{cm_i}) \cdot m_i c_i^2 \tag{52}$$

Where I_{GBCL_i} is the moment of inertia of link i with its corresponding counterweight respecting to joint i when excluding the effect of the successive links of link i; I_i is the moment of inertia of link i which respects to the center of mass of link i.

When including the effect of the successive links, the moment of inertia of link i can be expressed as (53).

$$I_{GBC_i} = I_i + (1 + \frac{m_i}{cm_i}) \cdot m_i c_i^2 + l_i^2 \cdot \sum_{j=i+1}^{n} (cm_j + m_j) \tag{53}$$

Where I_{GBC_i} is the moment of inertia of link i with its

corresponding counterweight respecting to joint i when including the effect of its successive links and their corresponding counterweights.

Because the counterweights eliminate the influence of self-weight of each constituent link of the manipulator, the gravitational force will not affect the dynamic performance of the manipulator any more. After the moment of inertia of each constituent link is conducted, the acceleration ellipsoid of a manipulator system which is equipped with counterweights can be expressed as (54).

$$(\ddot{x} + JM_{cw}^{-1}c_{cw} - \dot{J}\dot{q})^T Q_{cw}(\ddot{x} + JM_{cw}^{-1}c_{cw} - \dot{J}\dot{q}) \le 1 \qquad (54)$$

Where M_{cw} is the inertial matrix of the manipulator which includes the effect of the counterweights; c_{cw} is the vector of the torque caused by the centrifugal and Coriolis forces after the counterweights are applied; $Q_{cw} = J^{-T}M_{cw}^{T}L^{-T}L^{-1}M_{cw}J^{-1}$.

The acceleration radius of a manipulator after being equipped with a gravity balance mechanism based on the counterweight approach can be conducted by following the processes provided in Section 2.2.

After conducting the acceleration radiuses of a manipulator before and after being gravity balanced by using the counterweight approach, the dynamic performance variation resulted from the installation of the counterweights can be expressed by maneuverability ratio which is interpreted in Section 2.3.

3.2 The Dynamic Performance of a Manipulator after being Equipped with a Gravity Balance Mechanism Based on the Auxiliary Parallelogram Approach

When auxiliary parallelograms equip to a manipulator to achieve gravity balance, extra links are added to each constituent link of the manipulator and would result in the increase of the mass and moment of

inertia of the manipulator system, though this phenomenon is not significant in most of practical applications. For the auxiliary parallelogram approach, the auxiliary links are built to be parallel to the original corresponding link of the manipulator or vertical to the ground. The moment of inertia resulted from the auxiliary links can be expressed as (55).

$$I_{AL_i} = I_{p_i} + I_{h_i} + m_{p_i} c_{p_i}^2 + m_{h_i} c_{h_i}^2 \tag{55}$$

Where I_{AL_i} is the moment of inertia resulted from the auxiliary links of link i; I_{p_i} is the moment of inertia of link p_i respecting to the center of mass of link p_i; I_{h_i} is the moment of inertia of link h_i respecting to the center of mass of link h_i; link p_i is the link parallel to the gravitational direction and connects link i and link h_i; link h_i is the link parallel to link i and connects link p_i and link h_{i-1} or an inert joint; m_{p_i} and m_{h_i} are the masses of link p_i and link h_i respectively; c_{pi} and c_{hi} are the distance from the center of mass of link p_i to joint i and the distance from the center of mass of link h_i to joint i respectively.

For the auxiliary parallelogram approach, the auxiliary links are used to create an environment to compress or stretch the spring system to store or release elastic potential energy to compensate the variation in gravitational potential energy resulted from the posture change of the manipulator without considering the effect of the deformation of the auxiliary links on positioning accuracy. This means the auxiliary links do not need a stiff structure or strength so the mass of the each auxiliary link is relative small when comparing it with the one of the corresponding link of the manipulator in most of the practical applications. Based on this, eliminating the mass of auxiliary links would not result in significant

deviation when conducting the inertial matrix and dynamic performance of the manipulator system. The moment of inertia of link i with its corresponding auxiliary links and its successive links with their corresponding auxiliary links can be expressed as (56).

$$I_{A_i} = I_i + I_{p_i} + I_{h_i} + m_i c_i^2 + m_{p_i} c_{p_i}^2 + m_{h_i} c_{h_i}^2 + \sum_{j=i+1}^{n} (I_j + I_{p_j} + I_{h_j} + m_j l_{C_j}^2 \cdot + m_{p_j} l_{PC_j}^2 + m_{h_j} l_{HC_j}^2) \quad (56)$$

Where I_{A_i} is the moment of inertia of link i which includes the effect of the auxiliary and successive links; l_{C_j} is the distance between the center of mass of the successive link j and joint i; l_{PC_j} is the distance between the center of mass of the successive auxiliary link p_j and joint i; l_{HC_j} is the distance between the center of mass of the successive auxiliary link h_j and joint i.

Similar with what has been studied in Section 3.1, the influence of gravitational force is eliminated through using these auxiliary links. Thus, the acceleration ellipsoid of a manipulator which is equipping with auxiliary parallelograms can be expressed as (57).

$$(\ddot{x} + JM_{ap}^{-1} c_{ap} - \dot{J}\dot{q})^T Q_{ap} (\ddot{x} + JM_{ap}^{-1} c_{ap} - \dot{J}\dot{q}) \le 1 \quad (57)$$

Where M_{ap} is the inertial matrix of the manipulator which is equipped with the auxiliary parallelograms; c_{ap} is the vector of the torque caused by the centrifugal and Coriolis forces after the auxiliary parallelograms are applied; $Q_{ap} = J^{-T} M_{ap}^T L^{-T} L^{-1} M_{ap} J^{-1}$.

The acceleration radius of a manipulator after being equipped with a gravity balance mechanism based on the auxiliary parallelogram approach can be conducted by following the processes provided in Section 2.2.

After conducting the acceleration radiuses of a manipulator before and

after being gravity balanced by using the auxiliary parallelogram approach, the dynamic performance variation resulted from the installation of the auxiliary parallelograms can be expressed by maneuverability ratio which is interpreted in Section 2.3.

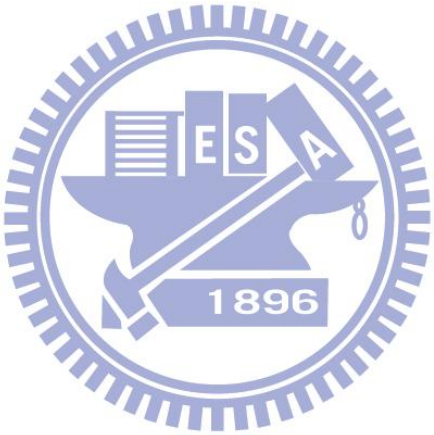

IV. Evaluate the Service Life of a Manipulator Including its Dynamic Performance

Manipulators used in industrial field usually have the requirements on the positioning accuracy, and sometime the requirements on dynamic performance are also shown in the specifications. To emphasize the importance of dynamic performance without losing the generality, this study assumes that the unacceptable outcome of a manipulator is defined as the positioning accuracy or dynamic performance of a manipulator is out of what is specified in its specification. Usually the positioning accuracy of a manipulator is dominated by the capability of its controllers and the deviation between the nominal dimensions of its constituent components and the real ones. In the following discussion, it assumes that the positioning accuracy is only affected by the length of each constituent link and the control accuracy of actuator controllers. Based on this assumption, the designed service life of a manipulator before and after being equipped with a gravity balance mechanism by using the counterweight or auxiliary parallelogram approach will be conducted in the following sections.

4.1 Service Life of a Manipulator

For a manipulator used in industrial field, it would have a certain specification to specify its positioning accuracy and dynamic performance, and this specification is the guideline for the users to plan how to use this manipulator. If a manipulator cannot fully satisfy what is specified in its specification, it means that what users plan to do according to this specification may not be achieved, and the users would consider that this manipulator fails. For most of the manipulators used in industrial field, the positioning accuracy or dynamic performance which is specified in the specifications is usually lower than what they really can achieve. This is because there are many factors cannot be fully controlled in the manufacturing processes and service environments. Meanwhile the

positioning accuracy and dynamic performance of a manipulator highly depends on its configuration and posture, and this makes it very difficult to designers of manipulators to evaluate the positioning accuracy and dynamic performance at each position and direction of the workspace which this manipulator can reach. However, users always think the performance specified in the specification is achievable when the manipulator performs that function. The difference on positioning accuracy or dynamic performance between the one specified in the specification and the designed one is used to be the safety margin of this manipulator. This margin is used to assure that even an unexpected adverse condition occurs, the manipulator still can fully satisfy what is specified in the specification. However, when the effect resulted from the adverse conditions is greater than what this safety margin can compensate, the manipulator cannot fully satisfy what is specified in its specification and fails.

However, the components used in a manipulator will age and wear with the time in service. After certain service time, the designed safety margin may not fully compensate the deterioration in positioning accuracy or dynamic performance resulted from these age and wear-out of the components in service. When this happens, this manipulator would not fully satisfy what is specified in its specification and makes the users unsatisfied. Based on the explanation above, this study defines the service life of a manipulator as: The time that the positioning accuracy and dynamic performance of a manipulator at certain service conditions is still under what is specified in its specification. This means the dissatisfaction or failure of a manipulator occurs when the positioning accuracy or dynamic performance of the manipulator deteriorates with the service time and out of what is specified in its specification. In lots of real occasions, the exact specification in positioning accuracy or dynamic performance of a manipulator is not known in the design phase, and it is a good practical way

that utilizes the specification or real performance of an existing manipulator to be the design specification of a manipulator which is in developing in the design phase.

Following the definition of the service life of a manipulator stated above, deterioration rate can be used as the design criterion on the dynamic performance of the manipulator which is used to verify whether the dynamic performance of a manipulator in developing is still under the design specification or still better than the comparative one after a certain service time. When the deterioration rate exceeds the tolerable deviation specified in the specification or worse than the worst performance of the comparative one, this means that this manipulator cannot guarantee that it can fully satisfy the dynamic requirements which are specified in its specification or be better than the performance that the users can accept now. In the above verification or comparison on dynamic performance of a manipulator after a certain service time is performed in the design phase, not the service life gained in experiments or gathered from the feedback of the users. Hence, this study sometime uses designed service life instead of service life. In this study, it assumes that if the deterioration rate of a manipulator is still smaller than the tolerable deviation in dynamic performance specified in the specification or better than the worst performance of the comparative one after a certain service time, the manipulator does not fail or can be accepted on its dynamic performance at that time.

Similarly, the designed service life of a manipulator on positioning accuracy can be defined as the time that the deviation between the designed and the real positioning is still under the design specification or is better than the comparative one. As what is explained above, only the age of actuator controllers and the wear-out of the constituent links will affect the positioning accuracy of a manipulator. This means the failure in the

positioning accuracy of a manipulator occurs when any error resulted from the age of controllers or the wear-out of links exceeds what is specified in the design specification or is worse than the corresponding one of the comparative manipulator.

4.2 The Failure Model of a Manipulator without Gravity Balance

For a manipulator, any its component or any functional performance which is out of the specification or worse than its comparative baseline would result in the whole system cannot fully satisfy what it should achieve and cause the failure of the manipulator system. Figure 9 shows the failure block diagram of a manipulator without gravity balance.

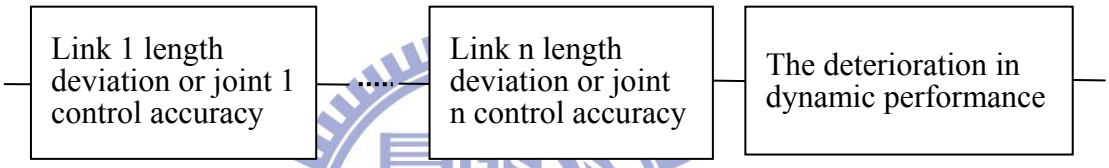

Figure 9: Failure block diagram of the original manipulator

From the above diagram, it is easy to find that the length of each link, the control capability of each joint actuator controller, or the dynamic performance of a manipulator is not under the specification or worse than its comparative baseline will cause the failure of the manipulator system. The deviation of the length of each constituent link during the operation is usually resulted from the wear-out of each corresponding joint, and the deterioration on control capability of each joint actuator controller is always caused by the age of controller itself. The deviation on the link length and the degradation on joint control capability will result in the deterioration of the positioning accuracy and dynamic performance of a manipulator. Following above explanation, the designed service life of a manipulator without gravity balance can be defined as the time of the first occurrence of any link length, any joint control accuracy, or dynamic performance of the manipulator is out of its design specification or worse

than the comparative baseline.

4.3 The Failure Model of a Gravity Balanced Manipulator by Utilizing the Counterweight Approach

Because a manipulator which counterweights equip to has almost the same configuration as the original one except the counterweights, it has the same failure block diagram as the one shown in Figure 9. Figure 10 shows the failure block diagram of a manipulator which is equipped with counterweights.

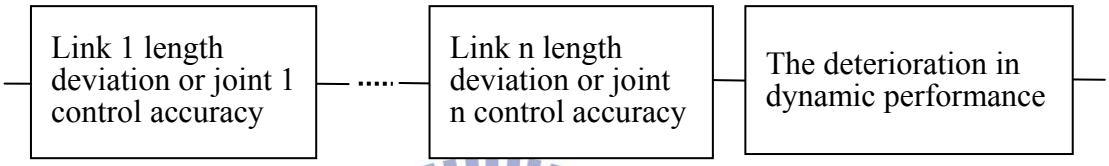

Figure 10: Failure block diagram of a manipulator which is equipped with counterweights

Although this diagram is fully the same as the one shown in Figure 9, the load and wear-out of each joint of the manipulator equipped with counterweights is different than the one without being gravity balanced. The designed service life of a manipulator which is equipped with counterweights should be different with the one without being gravity balanced.

4.4 The Failure Model of a Gravity Balanced Manipulator by Utilizing the Auxiliary Parallelogram Approach

When a manipulator is equipped with auxiliary parallelograms, extra links and joints will be added to it. According to the basic concept of design, more components would result in the system more complicated and easier to get glitch. However, these extra added links and joints will not make the manipulator system fail directly because the function of them is to eliminate the influence of the self-weight of the manipulator they apply. Because the auxiliary parallelograms belong to the passive mechanism,

there is no need to use controllers or actuators on them. When the wear-out increases the deviation of the length of each constituent link of the auxiliary parallelograms, their performance on eliminating the self-weight of the manipulator may deteriorate associatively and may worsen the dynamic performance of the manipulator when compares with the one without the deviation in the length of constituent links of the auxiliary parallelograms. For the worst case, when the equipped auxiliary parallelograms fully lose the function of eliminating self-weight, this manipulator still can satisfy the original positioning and dynamic requirements if the joint or link which fails does not obstruct any component of the original manipulator. This means that the auxiliary parallelograms will not affect the designed service life which is based on the functional performance on positioning and dynamic performance of a manipulator directly, but it will change the loading conditions on the constituent joints and also change the wear-out rate of these joints associatively. The failure block diagram of a manipulator which is equipped with auxiliary parallelograms is shown in Figure 11 which is the same as the ones shown in Figure 9 and Figure 10, respectively.

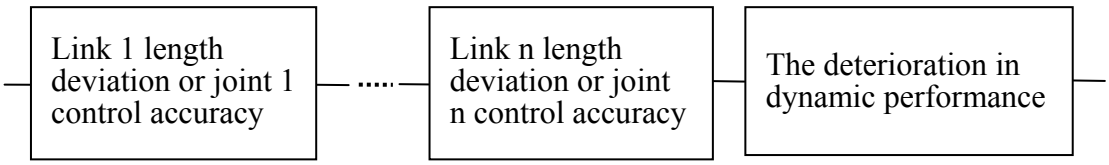

Figure 11: Failure block diagram of a manipulator equipping with parallelograms

V. Example

In this chapter, a PUMA 560 robot arm will be used as an example to demonstrate how to evaluate the variation in the dynamic performance and service life of a manipulator before and after being equipped with a gravity balance mechanism. Because the last three links of a PUMA 560 robot arm which compose the wrist are not used to achieve or satisfy any requirement on dynamic performance but are used to control the orientation of the object held by the end-effector, the last three links will be taken as a mass point on the end of the third link of the PUMA 560 robot arm in the following discussion. Meanwhile, the frictional force is omitted in the following discussion, and the workspace under discussion is the region which covers what is the most used in the pick and place applications [53]. It is also assumed that each auxiliary link is rigid and massless, and the maximum acceptable errors of the configuration of a PUMA 560 robot arm which are resulted from the manufacturing, assembling, and operating processes are the same as the ones used in case 1 of example 2 of [53].

Because the workspace of a PUMA 560 robot arm is almost axial symmetric to the axis of joint 0, there is no need to specify the angular position of joint 0 when discussing its positioning accuracy and dynamic performance under a certain workspace [53]. According to the literature [59], the average service life of an industrial robot arm is about 12 years. Based on what states above and what the errors are used in the literature to evaluate the deterioration of the dynamic performance due to these errors [53], the joint wear-out of a PUMA 560 robot arm without being gravity balanced after 12 years in service is assumed to be one thousandth of the corresponding link length, and the angular error resulted from the controller is assumed to be 0.1° after 12 years in service. Because the angular errors are resulted from the age of the controllers which belong to a kind of electronic product, the proliferation of the angular errors is assumed to be

in exponential. The wear-out of each joint is assumed that follows Archard wear model [60], and can be express as (58).

$$\frac{H}{S} = Kp \tag{58}$$

Where H is the wear depth, S is the relative sliding distance between the two bodies in contact, K is a wear coefficient, and p is the contact pressure which comes from the contact of the concerned bodies. In Archard wear model, it states that the quantity or wear depth of wear-out of a joint is proportional to the relative move distance of the two contact surface and the normal force it takes. Because all the manipulators under discussion are operated in the same conditions, this means that all the corresponding joints of these manipulators will have the same relative move distance and have the same age rate on their controllers. Consequently, the relationship of the wear depth of the wear-out between the corresponding joints is the same as the relationship of the normal force between the corresponding joints, and all the joints will have the same angular error due to the same age conditions of controllers.

In this example, the dynamic performance is calculated at the standing posture, and the positioning and dynamic performance of a PUMA 560 robot arm without being gravity balanced is the baseline of acceptance. When a PUMA 560 robot arm is equipped with a gravity balance mechanism, and its positioning accuracy or dynamic performance at a certain workspace after a certain time in service is worse than the worst one performed by a PUMA 560 robot arm without being gravity balanced during its service life, this means that the gravity balanced PUMA 560 robot arm cannot fully satisfy what the users need at this region after a certain time in service. When this phenomenon happens, the manipulator is defined as failure.

In the following discussion, one year will be taken as the time interval

to evaluate the deterioration in positioning accuracy and dynamic performance of a PUMA 560 robot arm which is resulted from the age of the controllers it equips and the wear-out of joints it is consisted of. The simulation period under discussion is from the start of the service to the end of the 12 years in service. Table 1 shows the errors resulted from age and wear-out of a PUMA 560 robot arm without being equipped with any gravity balance mechanism, after it is equipped with counterweights, and after it is equipped with auxiliary parallelograms at each time interval, respectively.

Summarily, the setup of this simulation can be listed as below:

1. Simulation subject: PUMA 560 robot arm
2. Only the counterweight and the auxiliary parallelogram approaches are discussed in the simulation.
3. Simulation is performed at standing posture and in a prescribed workspace or region.
4. The last three links are taken as a mass point at the end of link 3.
5. Auxiliary links are massless, and the friction effect is negligible.
6. The maximum acceptable angular error is 0.1^{o}, and the maximum acceptable length error is one thousandth of the corresponding nominal link length.
7. Angular error is resulted from the age of controllers, and the length error is caused by wear-out.
8. Angular error increases exponentially, and length error follows Archard wear model.
9. The service is 12 years.
10. Both positioning and dynamic performance are included in the acceptance criteria of a manipulator, and the performance baseline is the worst corresponding one performed by the manipulator without being gravity balanced.

Table 1 Angular and length errors of a PUMA 560 robot arm without being gravity balanced, after being equipped with counterweights, and after being equipped with auxiliary parallelograms

Time (year)	Angular error (^{o})	Length error of not gravity balanced (m)		Length error of using counterweights (m)		Length error of using parallelograms (m)	
		Link 1	Link 2	Link 1	Link 2	Link 1	Link 2
1	1.00e-12	3.58e-5	3.58e-5	1.72e-4	1.45e-4	6.49e-4	3.33e-4
2	1.00e-6	7.17e-5	7.17e-5	3.44e-4	2.90e-4	1.30e-3	6.66e-4
3	1.00e-4	1.08e-4	1.08e-4	5.15e-4	4.35e-4	1.95e-3	1.00e-3
4	1.00e-3	1.43e-4	1.43e-4	6.87e-4	5.80e-4	2.60e-3	1.33e-3
5	3.98e-3	1.79e-4	1.79e-4	8.59e-4	7.26e-4	3.24e-3	1.67e-3
6	1.00e-2	2.15e-4	2.15e-4	1.03e-3	8.71e-4	3.89e-3	2.00e-3
7	1.93e-2	2.51e-4	2.51e-4	1.20e-3	1.02e-3	4.54e-3	2.33e-3
8	3.16e-2	2.81e-4	2.81e-4	1.38e-3	1.16e-3	5.19e-3	2.66e-3
9	4.64e-2	3.23e-4	3.23e-4	1.55e-3	1.31e-3	5.84e-3	3.00e-3
10	6.31e-2	3.58e-4	3.58e-4	1.72e-3	1.45e-3	6.49e-3	3.33e-3
11	8.11e-2	3.94e-4	3.94e-4	1.89e-3	1.60e-3	7.14e-3	3.66e-3
12	0.10	0.00043	0.00043	0.00206	0.00174	0.00779	0.00400

From Table 1, it is easy to find that the wear-out of the PUMA 560 robot arm which is equipped with auxiliary parallelograms is greatest in these cases, and it is about 18 times of the quantity of the one without being gravity balanced. When the PUMA 560 robot arm is equipped with counterweights, its wear-out is still greater than the one without being gravity balanced, and it is about 5 times more. After further investigating into the wear-out of a PUMA 560 robot arm without or with being gravity balanced, it is found that the joints of the one which is equipped with auxiliary parallelograms bear the greatest normal force which is resulted from the auxiliary parallelograms and the corresponding springs. It is also found that the joints of the PUMA 560 robot arm which is equipped with counterweights still needs to bear greater normal force than the

corresponding ones without being gravity balanced. This is why the wear-out becomes more significant when a PUMA 560 robot arm is gravity balanced.

5.1 The Deterioration in Dynamic Performance of a PUMA 560 Robot Arm

The skeleton drawing with the attached frames of a PUMA 560 robot arm without being gravity balanced in the zero position is shown in Figure 12. The parameters of Denavit–Hartenberg transformation matrix of the PUMA 560 robot arm are shown in Table 2. Table 3 and Table 4 show the inertial properties of the robot arm, and the information of center of mass of each constituent link and the output limit of each joint actuator respectively [53]. In Figure 13, it shows the shape of the region under discussion.

In Figure 14, it shows the dynamic performance which is expressed in acceleration radius of the PUMA 560 robot arm without being gravity balanced over the prescribed workspace. Figure 19a, 20a,…,30a show the deterioration in dynamic performance which is expressed in deterioration rate resulted from the age of the controllers and the wear-out of the joints of the PUMA 560 robot arm without being gravity balanced after servicing for 1 year, 2 years,…, 12 years respectively.

From Figure 19a, 20a,…,30a, it is found that the dynamic performance deteriorates with the time in service, and it also can be found that the angle of joint 1 mainly controls the trend of the deterioration in dynamic performance in the early time in service. After certain time in service (about 4 years), the trend of the deterioration in dynamic performance is mainly controlled by the angle of joint 2.

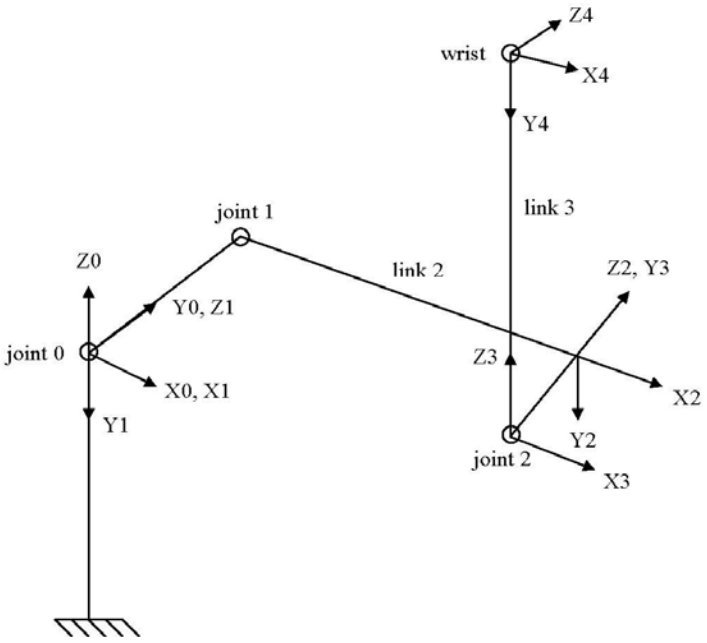

Figure 12: Zero position with attached frames of a PUMA 560 robot arm

Table 2 D-H parameters of the first three links of a PUMA 560 robot arm

Frame i	d_i [m]	θ_i [°]	a_i [m]	α_i [°]
1	0	θ_1	0	-90
2	0.2435	θ_2	0.4318	0
3	-0.0934	θ_3	0	90
4	0.4331	θ_4	-0.0203	-90

Table 3 Inertial parameters of a PUMA 560 robot arm

Link i	M [kg]	I_{xx} [kg-m^2]	I_{yy} [kg-m^2]	I_{zz} [kg-m^2]	$I_{xy}=I_{yz}=I_{zx}$ [kg-m^2]
1	0	0	0	0.35	0
2	17.4	0.13	0.524	0.539	0
3	4.8	0.066	0.0125	0.086	0
wrist	1.25	0	0	0	0

Table 4 Information of center of masses of the first three links and the corresponding output limits of the joint actuators

Link i	r_x [m]	r_y [m]	r_z [m]	Torque Limit [N-m]
1	0	0	0	±97.6
2	0.068	0.006	0.2275	±186.4
3	0	-0.070	-0.0794	±89.4
wrist	0	-0.0203	0.4141	-

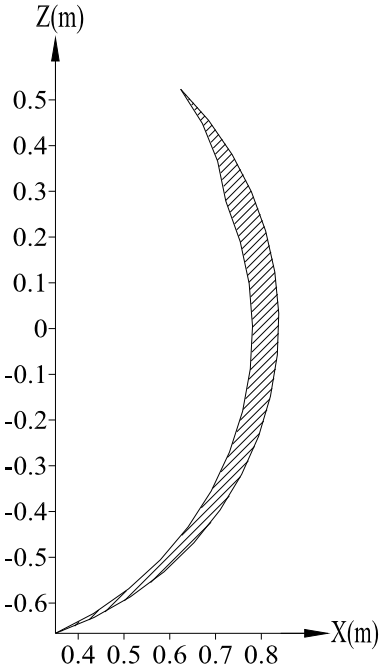

Figure 13: Workspace under discussion

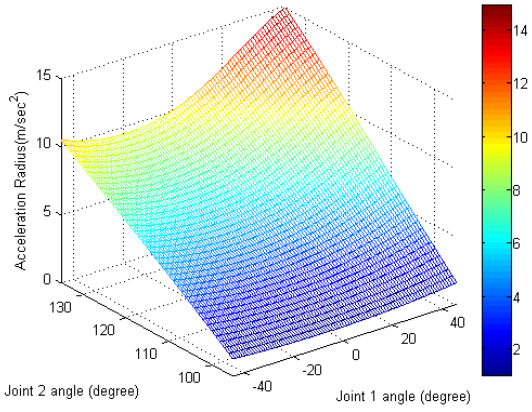

Figure 14: Dynamic Performance of a PUMA 560 robot arm without being equipped with any gravity balance mechanism

5.2 The Deterioration in Dynamic Performance of a PUMA 560 Robot Arm after the Counterweight Approach is Applied

Because the axis of the first joint, joint 0, is parallel to the gravitational direction, the gravitational force does not cause any torque to this joint actuator, and the gravity balance mechanism does not need to be

applied to this joint. Figure 15 shows the skeleton drawing of the PUMA 560 robot arm which is equipped with the counterweights. The corresponding parameters of the counterweights are shown in Table 5. The variation in dynamic performance which is expressed in maneuverability ratio of the PUMA 560 robot arm after being equipped with the counterweights is shown in Figure 16, and the dynamic performance deterioration after servicing for 1 year, 2 years,…, 12 years are shown in Figure 19b, Figure 20b,…, Figure 30b respectively.

From Figure 16, it is found that the dynamic performance of the PUMA 560 robot arm which is equipped with the counterweights is significantly worse than the one without being gravity balanced. From this figure, it can also be found that using maneuverability ratio can provide a better visual feeling and information to express the variation in the dynamic performance of a manipulator. After further investigating into the cause of this phenomenon, it is found that the counterweights which are equipped significantly increase the moment of inertia of each link, and this makes the dynamic performance of a PUMA 560 robot arm worse than the one without being gravity balanced. From Figure 19b, 20b,…,30b, it is found that the dynamic performance deteriorates with the time in service, and it is also found that the angle of joint 1 mainly controls the trend of the deterioration in dynamic performance in the early time in service. After certain time in service (about 7 years), the trend of the deterioration in dynamic performance is mainly controlled by the angle of joint 2.

Table 5 Parameters corresponding to the counterweights

Counterweight [kg]		Distance [m]	
mc_1	mc_2	wc_1	wc_2
70.62	18.45	0.2	0.05

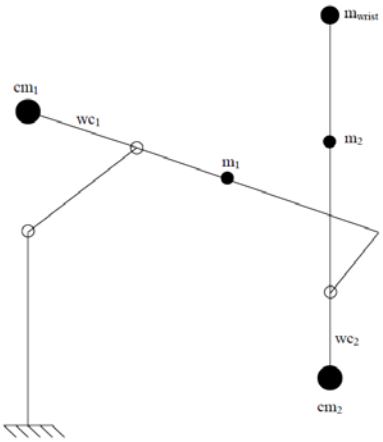

Figure 15: Skeleton drawing of a PUMA 560 robot arm which is equipped with the counterweights

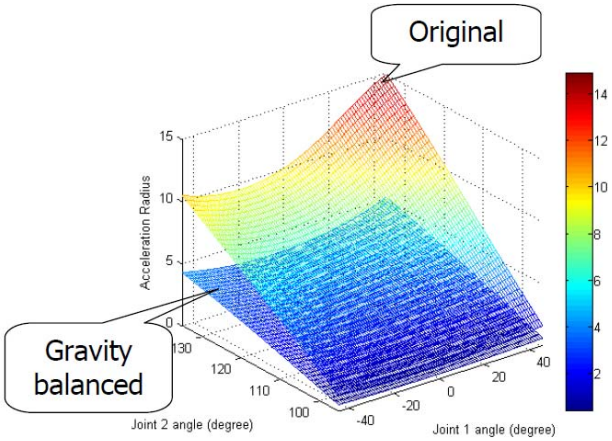

(a)

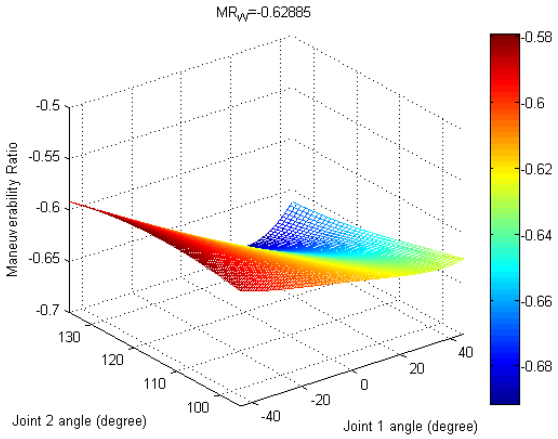

(b)

Figure 16: (a) Dynamic performance of a PUMA 560 robot arm before and after being equipped with the counterweights (b) Maneuverability ratio of a PUMA 560 robot arm equipped with the counterweights

5.3 The Deterioration in Dynamic Performance of a PUMA 560 Robot Arm after the Auxiliary Parallelogram Approach is Applied

The skeleton drawing of the PUMA 560 robot arm which is equipped with the auxiliary parallelograms is shown in Figure 17, and the corresponding parameters of the auxiliary parallelograms are shown in Table 6. The dynamic performance which is expressed in maneuverability ratio of the PUMA 560 robot arm which is equipped with the auxiliary parallelograms is shown in Figure 18, and the deterioration in dynamic performance after servicing for 1 year, 2 years,…, 12 years are shown in Figure 19c, Figure 20c,…, Figure 30c respectively.

From Figure 18, it is found that the dynamic performance of the PUMA 560 robot arm which is equipped with the auxiliary parallelograms is moderately better than the one without being gravity balanced. It can also be found that maneuverability ratio can provide the information of the variation in the dynamic performance of a manipulator even the variation is very small. After further investigating into this phenomenon, it is found that the bottle neck of the dynamic performance of a PUMA 560 robot arm falls on the output capacity of the actuator used in joint 0. Because joint 0 is not affected by the self-weight of a PUMA 560 robot arm, its loading will not be mitigated after the PUMA 560 robot arm is gravity balanced. This is why the dynamic performance of a PUMA 560 robot arm gets moderately improvement after being gravity balanced by the auxiliary parallelogram approach. From Figure 19c, 20c,…,30c, it is found that the dynamic performance deteriorates with the time in service, and it also can be found that the trend of the deterioration in dynamic performance in the early time in service is controlled by the angles of joint 1 and joint 2. After certain time in service (about 9 years), the trend of the deterioration in dynamic performance is mainly controlled by the angle of joint 2. One phenomenon should be noticed, and that is the deterioration in dynamic

performance at the period of 6 to 8 years in service is better than the one after 5 years in service. After further investigating into this, it is found that the trend of the deterioration in the dynamic performance of the PUMA 560 robot arm which is equipped with the auxiliary parallelograms is in the transition of that the trend of the deterioration in the dynamic performance is controlled by the angles of joint 1 and joint 2 to be mainly controlled by the angle of joint 2 during the period of 6 to 8 years in service. Though the deterioration in dynamic performance of the PUMA 560 robot arm after 6 to 8 years in service is worse than the one after 5 years in service in the majority of the region under discussion, but the minority of the region with higher deterioration rate, DR_P dominates the value of the representative index of the dynamic performance deterioration of this region, DR_W .

Because the trend of the distribution of deterioration rate changes in the period of 6 to 8 years in service, the subtle relationship between the errors and the deterioration in the dynamic performance of a PUMA 560 robot arm which is equipped with auxiliary parallelograms must also change in this period. During this transition, the value of DR_W is mainly controlled by the minority region with higher deterioration rate, DR_P and shows an unexpected trend. In the future studying, the detail of the mechanism which causes the change in the trend of the distribution of deterioration in the dynamic performance of a manipulator and the deterioration rate, DR_W , with some modification which can eliminate the influence of the minority region with higher deterioration rate, DR_P , should be investigated.

Table 6 Parameters corresponding to the auxiliary parallelograms

Auxiliary link length [m]				Stiffness coefficient of spring [N/m]	
lp_1	lc_1	lp_2	lc_2	k_1	k_2
0.2	0.3	0.2	0.2	1074.34	220.42

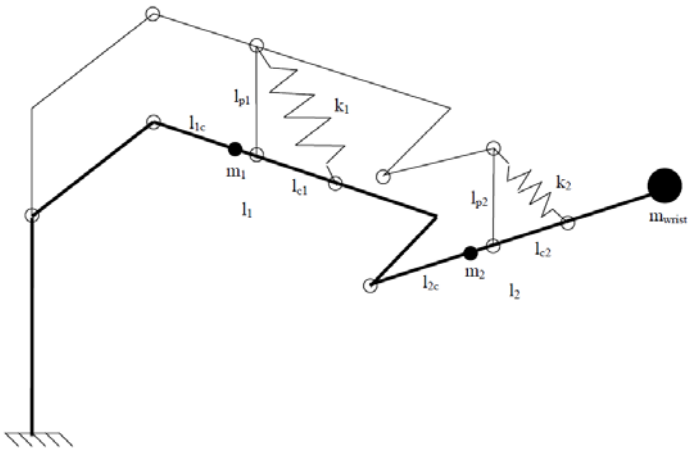

Figure 17: Skeleton drawing of a PUMA 560 robot arm which is equipped with the auxiliary parallelograms

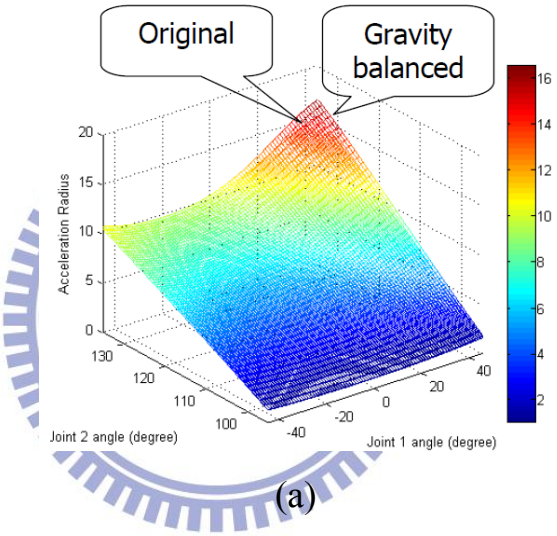

(a)

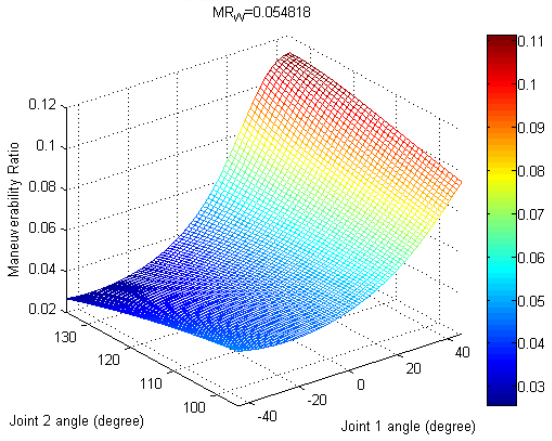

(b)

Figure 18: (a) Dynamic performance of a PUMA 560 robot arm before and after being equipped with the auxiliary parallelograms (b) Maneuverability ratio of a PUMA 560 robot arm equipped with the auxiliary parallelograms

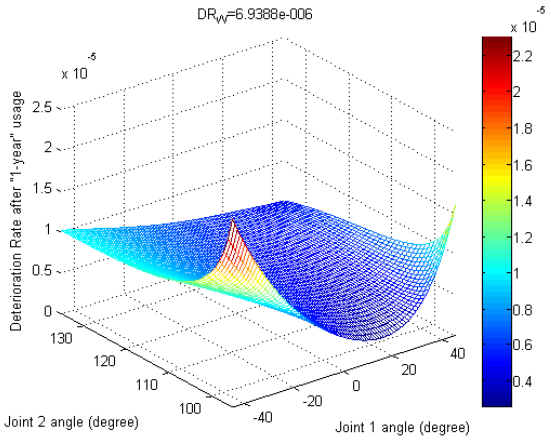

The trend of the deterioration in the dynamic performance is mainly controlled by the angle of joint 1.

(a)

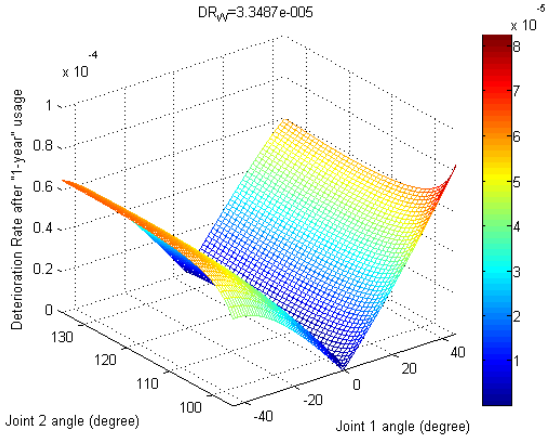

The trend of the deterioration in the dynamic performance is mainly controlled by the angle of joint 1.

(b)

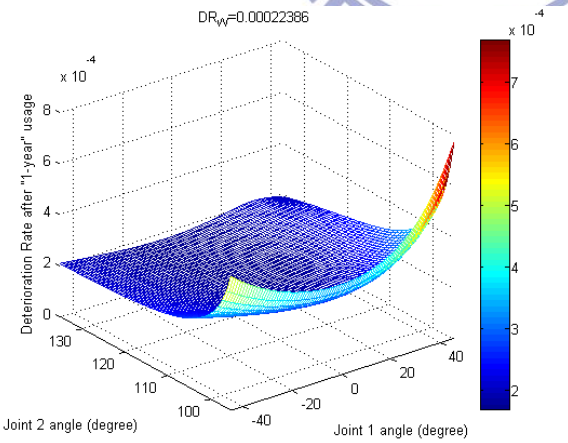

The trend of the deterioration in the dynamic performance is controlled by the angles of joint 1 and joint 2.

(c)

Figure 19: The deterioration in dynamic performance of a PUMA 560 robot arm after servicing for 1 year (a) without being gravity balanced (b) after being equipped with the counterweights (c) after being equipped with the auxiliary parallelograms

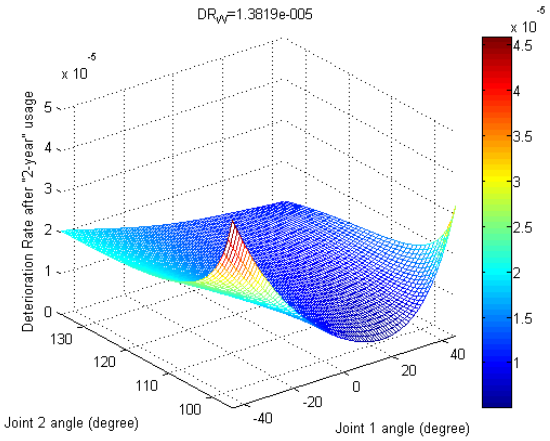

The trend of the deterioration in the dynamic performance is mainly controlled by the angle of joint 1.

(a)

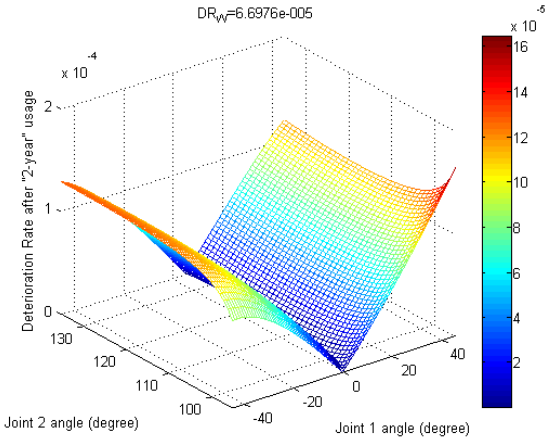

The trend of the deterioration in the dynamic performance is mainly controlled by the angle of joint 1.

(b)

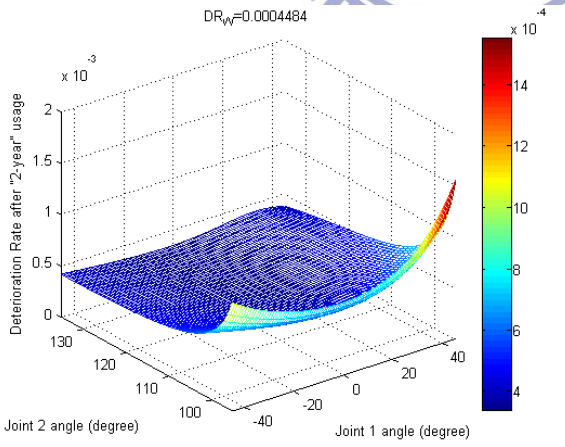

The trend of the deterioration in the dynamic performance is controlled by the angles of joint 1 and joint 2.

(c)

Figure 20: The deterioration in dynamic performance of a PUMA 560 robot arm after servicing for 2 years (a) without being gravity balanced (b) after being equipped with the counterweights (c) after being equipped with the auxiliary parallelograms

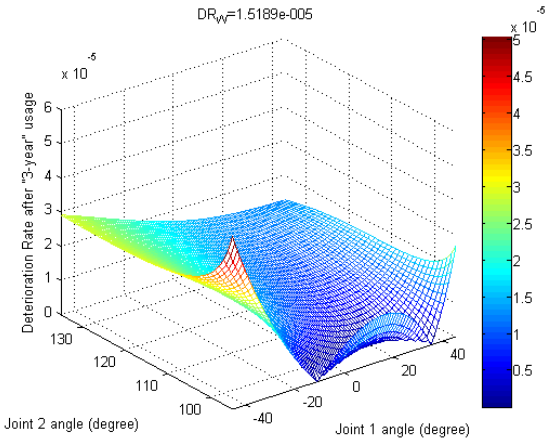

The trend of the deterioration in the dynamic performance starts to change but is still mainly controlled by the angle of joint 1.

(a)

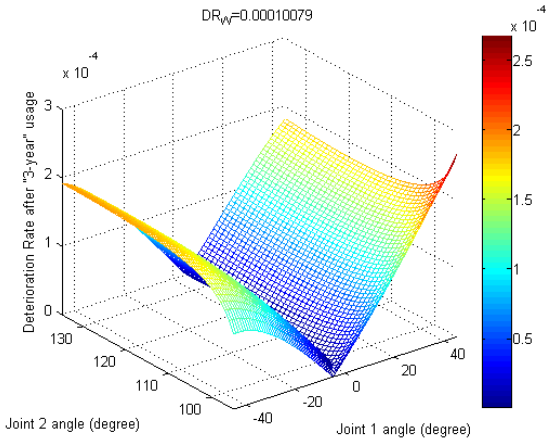

The trend of the deterioration in the dynamic performance is mainly controlled by the angle of joint 1.

(b)

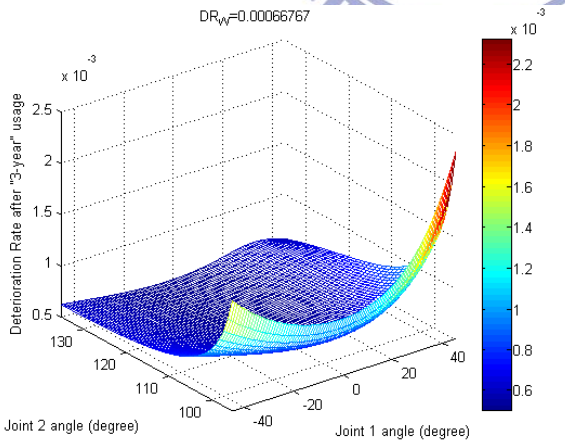

The trend of the deterioration in the dynamic performance is controlled by the angles of joint 1 and joint 2.

(c)

Figure 21: The deterioration in dynamic performance of a PUMA 560 robot arm after servicing for 3 years (a) without being gravity balanced (b) after being equipped with the counterweights (c) after being equipped with the auxiliary parallelograms

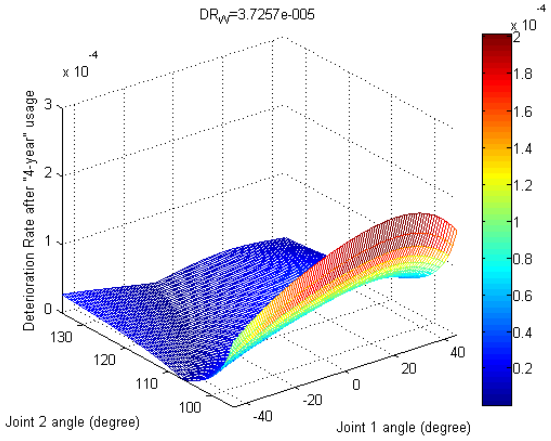

The trend of the deterioration in the dynamic performance is mainly controlled by the angle of joint 2.

(a)

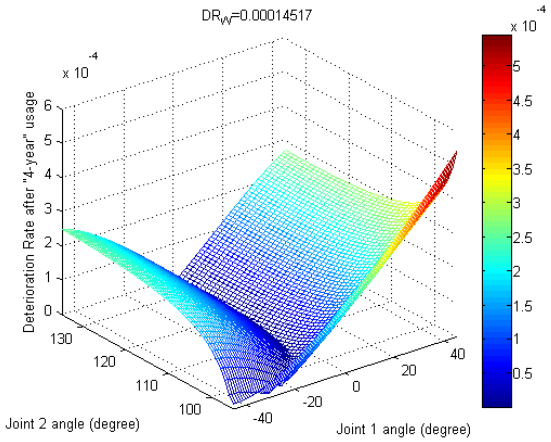

The trend of the deterioration in the dynamic performance starts to change but is still mainly controlled by the angle of joint 1.

(b)

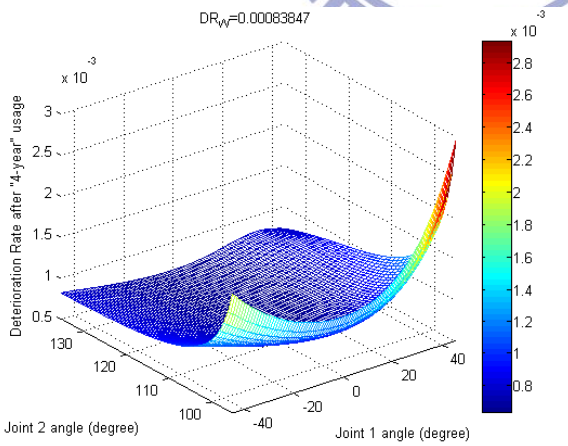

The trend of the deterioration in the dynamic performance is controlled by the angles of joint 1 and joint 2.

(c)

Figure 22: The deterioration in dynamic performance of a PUMA 560 robot arm after servicing for 4 years (a) without being gravity balanced (b) after being equipped with the counterweights (c) after being equipped with the auxiliary parallelograms

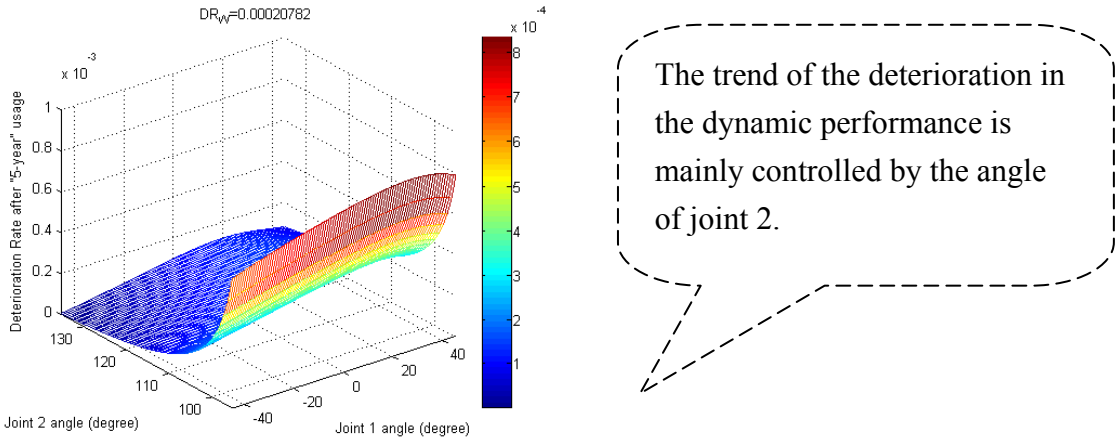

(a)

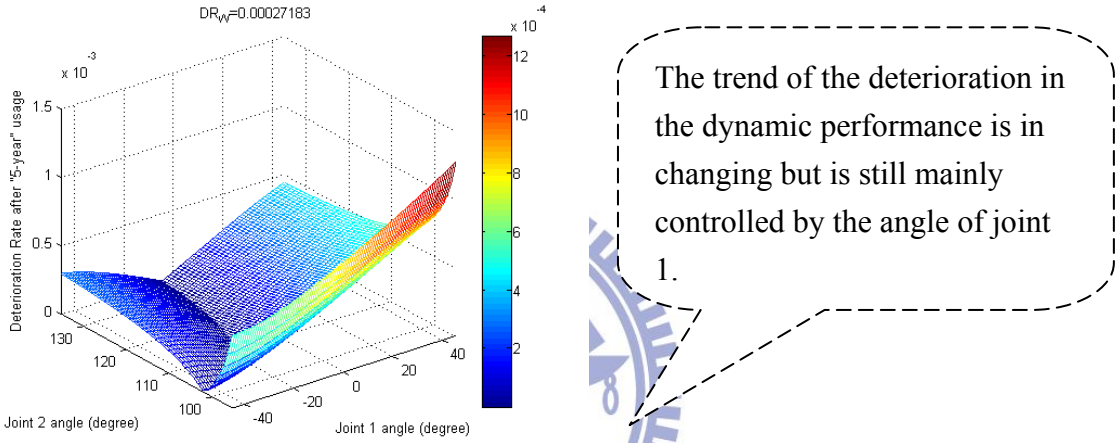

(b)

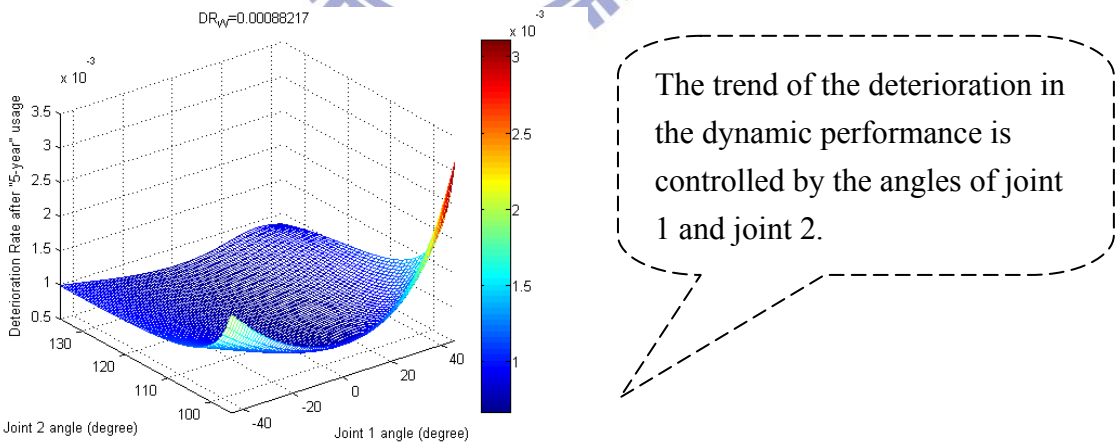

(c)

Figure 23: The deterioration in dynamic performance of a PUMA 560 robot arm after servicing for 5 years (a) without being gravity balanced (b) after being equipped with the counterweights (c) after being equipped with the auxiliary parallelograms

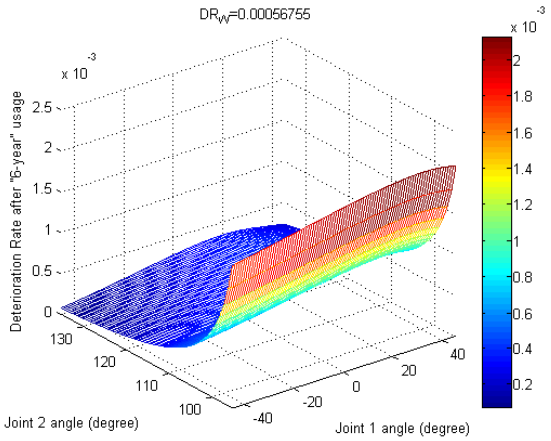

The trend of the deterioration in the dynamic performance is mainly controlled by the angle of joint 2.

(a)

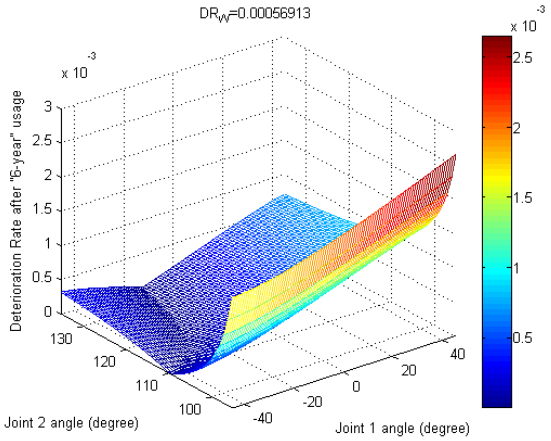

The trend of the deterioration in the dynamic performance is in changing but is controlled by the angles of joint 1 and joint 2.

(b)

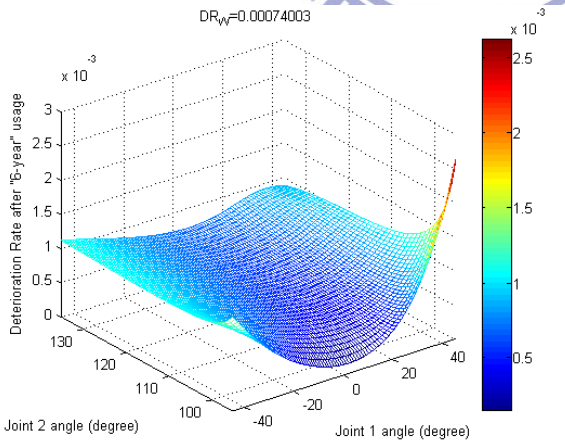

The trend of the deterioration in the dynamic performance starts to change and is controlled by the angles of joint 1 and joint 2.

(c)

Figure 24: The deterioration in dynamic performance of a PUMA 560 robot arm after servicing for 6 years (a) without being gravity balanced (b) after being equipped with the counterweights (c) after being equipped with the auxiliary parallelograms

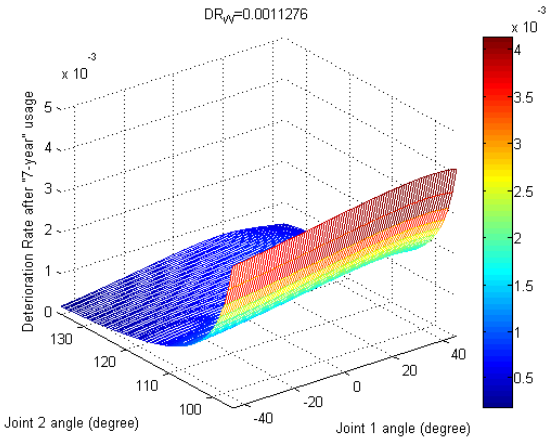

The trend of the deterioration in the dynamic performance is mainly controlled by the angle of joint 2.

(a)

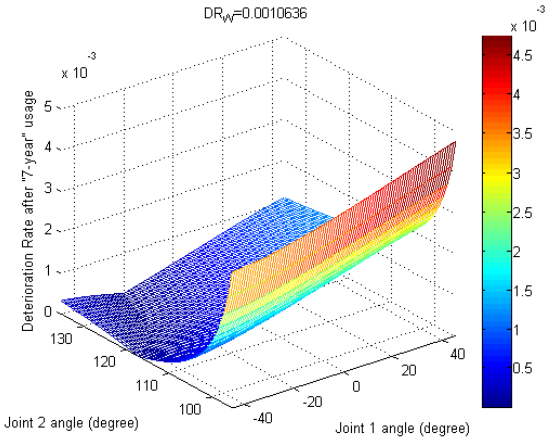

The trend of the deterioration in the dynamic performance is mainly controlled by the angle of joint 2.

(b)

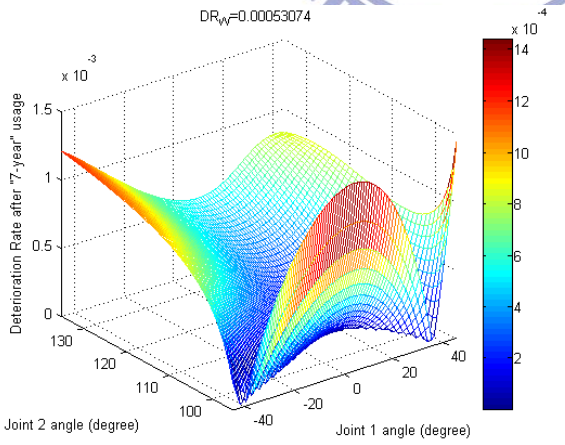

The trend of the deterioration in the dynamic performance is in changing and is still controlled by the angles of joint 1 and joint 2.

(c)

Figure 25: The deterioration in dynamic performance of a PUMA 560 robot arm after servicing for 7 years (a) without being gravity balanced (b) after being equipped with the counterweights (c) after being equipped with the auxiliary parallelograms

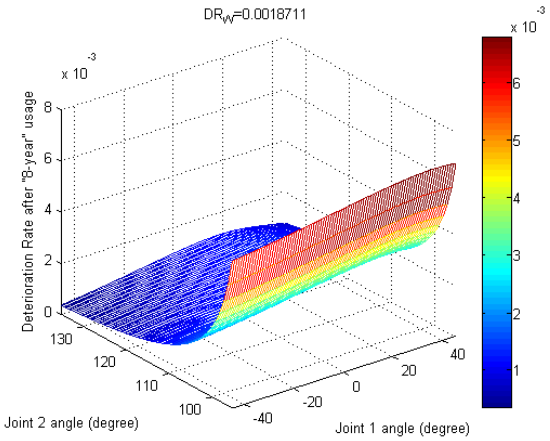

The trend of the deterioration in the dynamic performance is mainly controlled by the angle of joint 2.

(a)

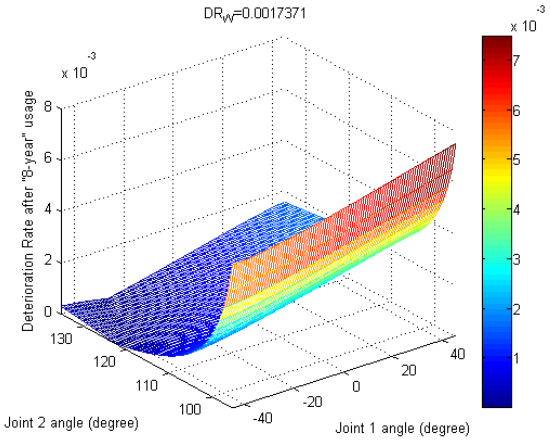

The trend of the deterioration in the dynamic performance is mainly controlled by the angle of joint 2.

(b)

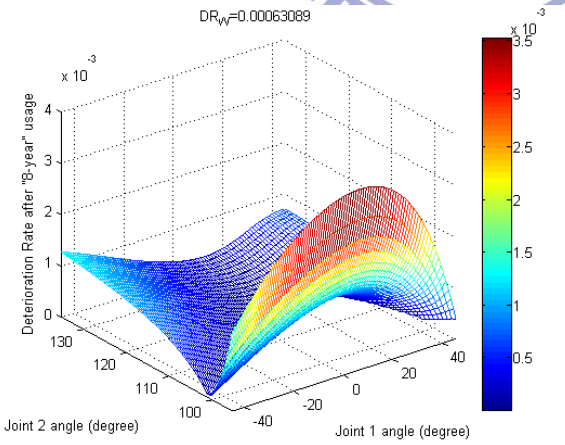

The trend of the deterioration in the dynamic performance is in changing and is still controlled by the angles of joint 1 and joint 2.

(c)

Figure 26: The deterioration in dynamic performance of a PUMA 560 robot arm after servicing for 8 years (a) without being gravity balanced (b) after being equipped with the counterweights (c) after being equipped with the auxiliary parallelograms

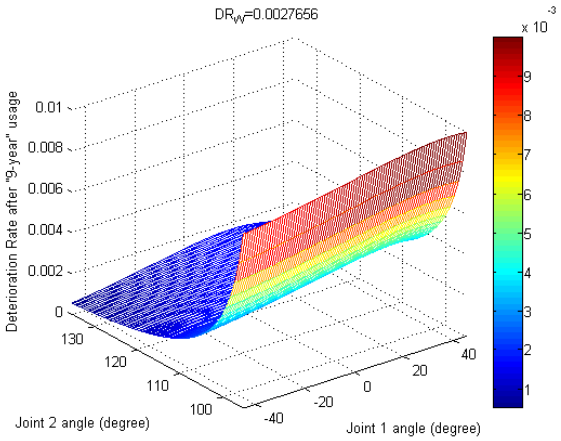

The trend of the deterioration in the dynamic performance is mainly controlled by the angle of joint 2.

(a)

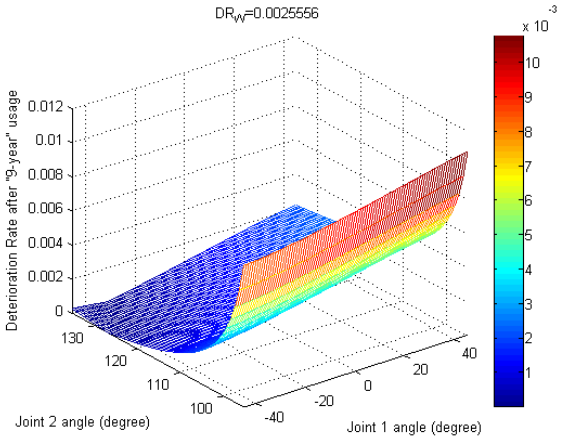

The trend of the deterioration in the dynamic performance is mainly controlled by the angle of joint 2.

(b)

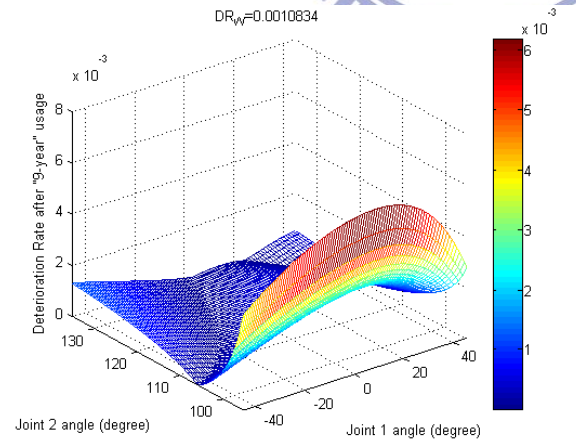

The trend of the deterioration in the dynamic performance is in changing and starts to be mainly controlled by the angle of joint 2.

(c)

Figure 27: The deterioration in dynamic performance of a PUMA 560 robot arm after servicing for 9 years (a) without being gravity balanced (b) after being equipped with the counterweights (c) after being equipped with the auxiliary parallelograms

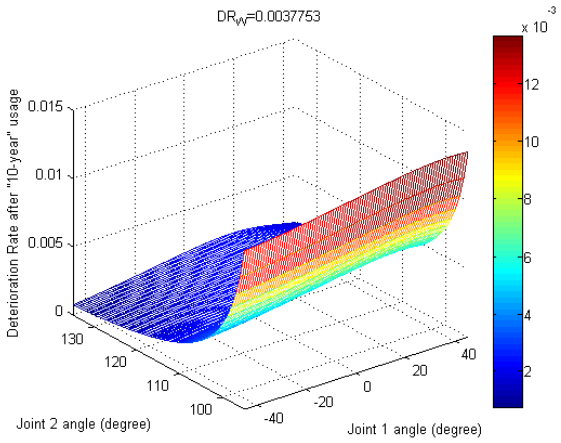

The trend of the deterioration in the dynamic performance is mainly controlled by the angle of joint 2.

(a)

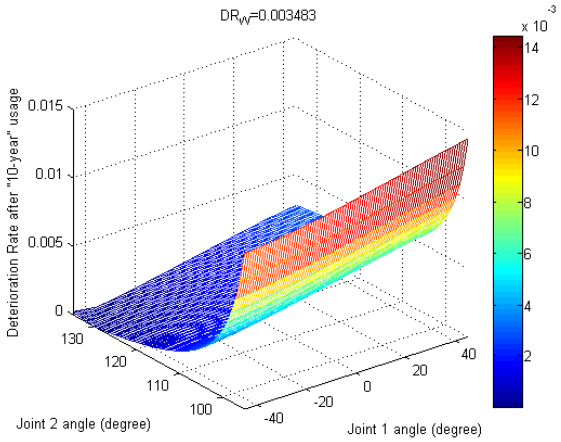

The trend of the deterioration in the dynamic performance is mainly controlled by the angle of joint 2.

(b)

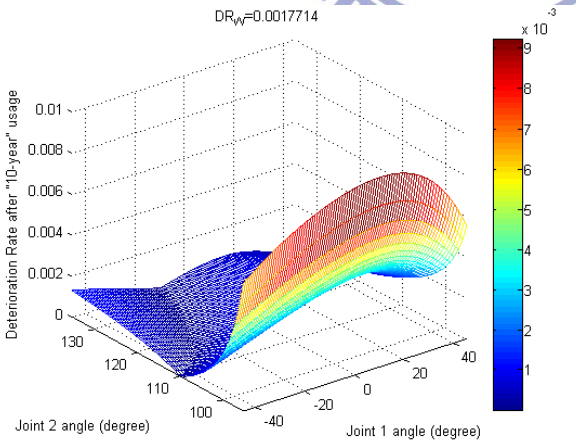

The trend of the deterioration in the dynamic performance is mainly controlled by the angle of joint 2.

(c)

Figure 28: The deterioration in dynamic performance of a PUMA 560 robot arm after servicing for 10 years (a) without being gravity balanced (b) after being equipped with the counterweights (c) after being equipped with the auxiliary parallelograms

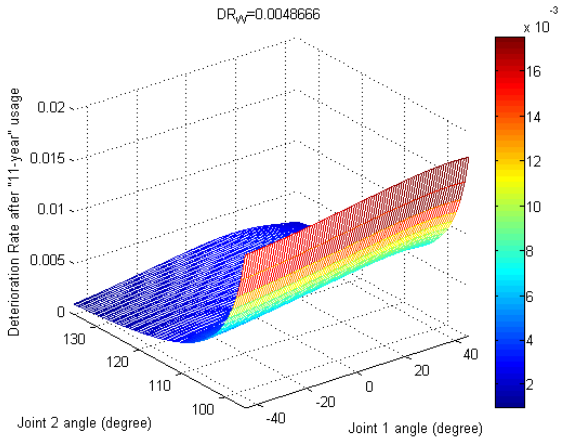

The trend of the deterioration in the dynamic performance is mainly controlled by the angle of joint 2.

(a)

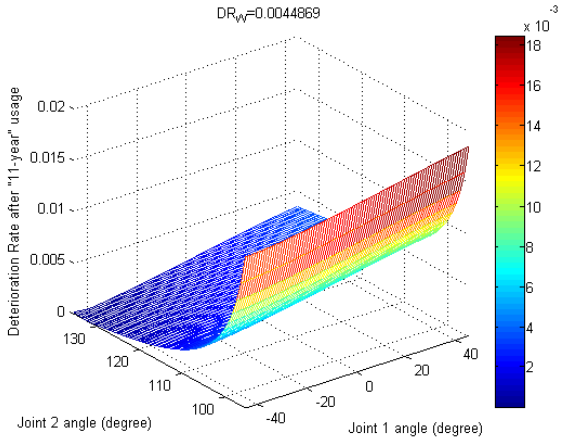

The trend of the deterioration in the dynamic performance is mainly controlled by the angle of joint 2.

(b)

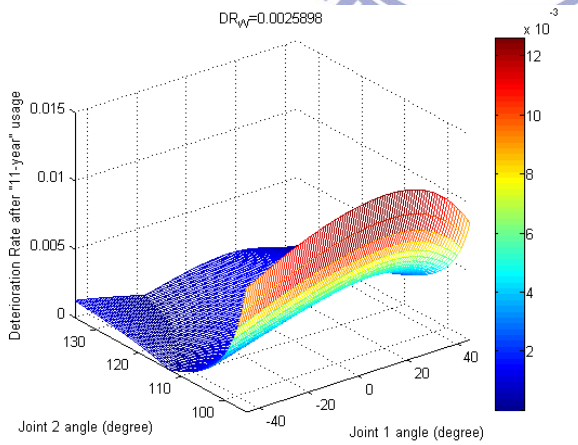

The trend of the deterioration in the dynamic performance is mainly controlled by the angle of joint 2.

(c)

Figure 29: The deterioration in dynamic performance of a PUMA 560 robot arm after servicing for 11 years (a) without being gravity balanced (b) after being equipped with the counterweights (c) after being equipped with the auxiliary parallelograms

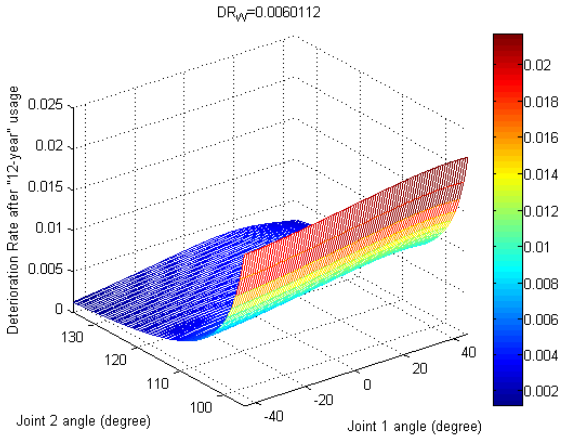

The trend of the deterioration in the dynamic performance is mainly controlled by the angle of joint 2.

(a)

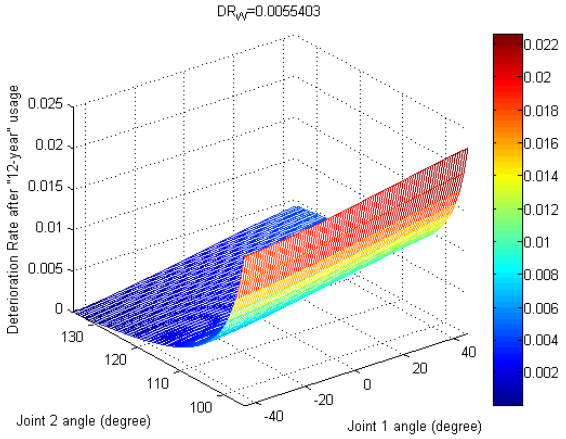

The trend of the deterioration in the dynamic performance is mainly controlled by the angle of joint 2.

(b)

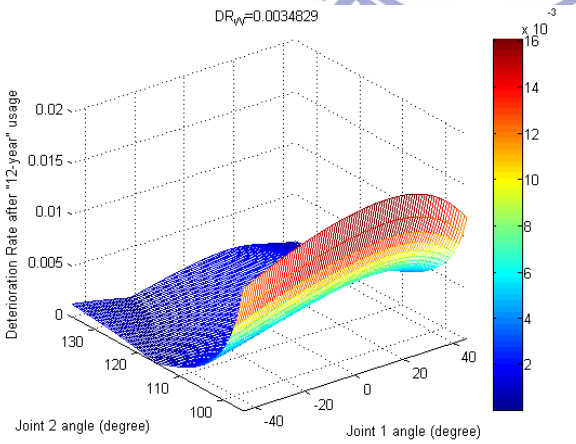

The trend of the deterioration in the dynamic performance is mainly controlled by the angle of joint 2.

(c)

Figure 30: The deterioration in dynamic performance of a PUMA 560 robot arm after servicing for 12 years (a) without being gravity balanced (b) after being equipped with the counterweights (c) after being equipped with the auxiliary parallelograms

5.4 Service Life of a PUMA 560 Robot Arm after being Gravity Balanced

From Figure 16, it is found that the dynamic performance of a PUMA 560 robot arm degrades significantly after the counterweight approach is applied. When the PUMA 560 robot arm is equipped with the auxiliary parallelograms, its dynamic performance gets moderate improvement according to Figure 18. From Figure 19 to Figure 30, the dynamic performance of a PUMA 560 robot arm without or with being gravity balanced deteriorates with the increase of the time in service except the one equipped with the auxiliary parallelograms after servicing for 6, 7, and 8 years.

From Table 1, it is easy to find that the length errors of the constituent links which are caused by the wear-out of the PUMA 560 robot arm which is equipped with counterweights excesses the maximum allowable error limit, 0.00043m, after 3 years in service. Meanwhile, the one equipped with the auxiliary parallelograms exceeds this limit just in the 1st year in service.

When the dynamic performance of a PUMA 560 robot arm without being gravity balanced is the acceptance baseline of dynamic performance at delivering, it is obvious that the one equipped with the counterweights is not acceptable because its designed dynamic performance is 62.885% worse than that criterion. For the one equipped with the auxiliary parallelograms, it is acceptable because its designed dynamic performance is slightly better than the criterion.

In Figure 31, it shows the run chart of the deterioration in the dynamic performance of the PUMA 560 robot arm without being gravity balanced, equipped with the counterweights, and equipped with the auxiliary parallelograms with the time in service. From this figure, it is found that the maximum deterioration in the dynamic performance of a PUMA 560 robot arm which is equipped with the counterweights is 0.554%, and the one

equipped with the auxiliary parallelograms is 0.348%. Both of them are better than the maximum one of a PUMA 560 robot arm without being gravity balanced. If the acceptance criterion is the maximum deterioration in the dynamic performance of a PUMA 560 robot arm without being gravity balanced, the gravity balanced PUMA 560 robot arms by utilizing the counterweight and auxiliary parallelogram approaches both are accepted.

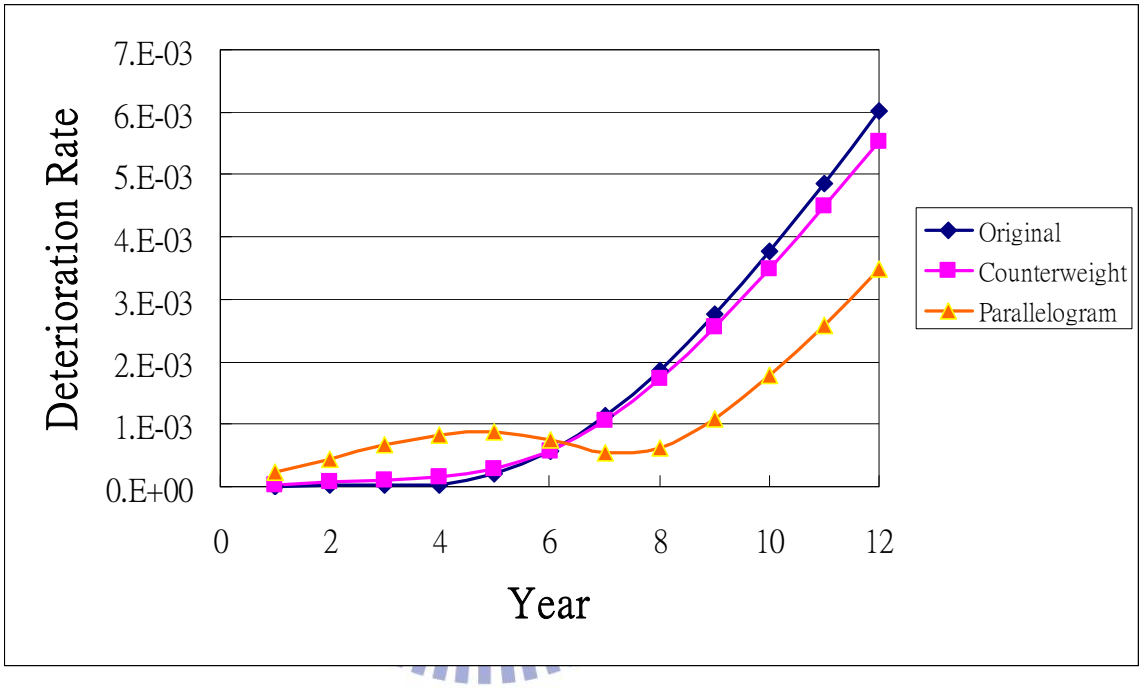

Figure 31: The run chart of the deterioration in the dynamic performance of a PUMA 560 robot arm without and with gravity balanced

When the worst positioning accuracy which can be represented by the length errors of constituent links or the joint angle errors of a PUMA 560 robot arm without being gravity balanced is the acceptance baseline, this means the one equipped with the counterweights fails in the 3rd servicing year, and the one equipped with the auxiliary parallelograms fails in its 1st servicing year. This implies that equipping gravity balance mechanisms to PUMA 560 robot arms would decrease designed service life of the robot arms because it increases the deterioration in positioning accuracy.

If the dynamic performance and the positioning accuracy all belong to

the acceptance criteria at delivering, only the one equipped with the auxiliary parallelograms with more aggressive maintenance plan is acceptable because of its greater wear-out in joints. This implies that if a PUMA 560 robot arm without being gravity balanced needs to be maintained every 12 years, the one equipped with the auxiliary parallelograms needs to be maintained about every 8 months or less. This makes a PUMA 560 robot arm equipped with the auxiliary parallelograms is suitable to be applied to the applications that the energy consumption and the dynamic performance are needed to be seriously concerned, but an aggressive maintenance plan is feasible and acceptable.

A PUMA 560 robot arm equipped with the counterweights is suitable to be applied to the applications that the energy consumption is the only one needs to be concerned and the dynamic performance is a very minor issue, but a conservative maintenance plan is feasible and acceptable.

A PUMA 560 robot arm without being gravity balanced is suitable to the applications that the energy consumption is a minor issue, and the dynamic performance and the service life are the issues need to be concerned.

VI. Conclusions

Gravity balance mechanisms can help a manipulator consume less energy and reduce the output requirements on the constituent actuators when this manipulator is used in static and low-speed applications. In many practical applications, manipulators not only must achieve certain positioning accuracy but also have to satisfy many requirements on the dynamic performance. However, in industrial field, the functional performance of a product is not the only criterion which needs to be considered. The service life of a product has the same importance level as the functions it can perform. Without proper data or methods to evaluate or compare the service life of a product, this product will be hard to be adopted or accepted in industrial field even if its functional performance is much better than the similar ones in use. To rectify this insufficiency, this article utilizes acceleration radius as the measure to evaluate the dynamic performance of a manipulator and uses maneuverability ratio to measure the dynamic performance variation of a manipulator before and after being equipped with a gravity balance mechanism. Deterioration rate is used in this study as the index to measure the degradation on dynamic performance of a manipulator with the time it serves. This study proposes a systematic approach that can be used to evaluate the variation and the deterioration in the dynamic performance of a manipulator before and after it is equipped with a gravity balance mechanism by using the indices stated above. An evaluation model is also proposed by this study which can include the effects of positioning and dynamic performance of a manipulator to roughly evaluate the service life after it is equipped with a gravity balance mechanism.

This study briefly interprets the fundamentals of the gravity balance approaches and the dynamic performance of manipulators. Two of the most practical gravity balance approaches, the counterweight and the auxiliary

parallelogram approaches, are chosen to discuss the influence of the gravity balance mechanisms on the dynamic performance and service life of a manipulator. In the example, it is easy to deduce that the counterweight approach can eliminate the influence of the self-weight of a PUMA 560 robot arm but also significantly decreases its dynamic performance. For the auxiliary parallelogram approach, it not only eliminates the influence of the self-weight of a PUMA 560 robot arm but also improves its dynamic performance. For both of these two approaches, they both alleviate the dynamic performance deterioration with the time in service, but the wear-out resulted from these two approaches become worse than the one without being gravity balanced.

From the simulation, it can be observed that the auxiliary parallelogram approach can not only eliminate the self-weight influence of a PUMA 560 robot arm but also improve its dynamic performance with less dynamic deterioration with the time in service. However, this approach will decrease the service life of a PUMA 560 robot arm resulted from the excessive wear-out which significantly degrades the positioning performance, and an aggressive maintenance plan is needed if the joints are not replaced by the better ones.

Summarily, the contribution of this study can be shown as below:

1. Provide the methodology to evaluate the influence of gravity balance mechanisms on the dynamic performance of a manipulator.
2. Provide a model which can be used to roughly evaluate the service life of a manipulator which includes the effects of positioning and dynamic performance.
3. Help designers of manipulators judge whether using gravity balance mechanisms to eliminate the influence of self-weight of a manipulator is beneficial to the application or not, to adjust the

setup of the controller which is used to perform the trajectory planning automatically after a gravity balance mechanism is applied, to conduct the new maintenance plan, and to identify which component would be the most critical one to the service life.

4. Help designers of manipulators evaluate which kind of gravity balance mechanism will be most beneficial to a given application, which maintenance plan may keep the manipulator performing its functions properly with maximum confidence and minimum cost, and which component should be revised to get better service life with minimum cost.

To get better understanding and investigate the subject of this study more thoroughly, the future studying will focus on the following directions:

1. Further investigate into the model of how configuration errors influence the dynamic performance of a manipulator after being gravity balanced and conduct a more precise mathematical model to explain the relationship between them in detail.
2. Conduct a reliability model based on the functional performance of a manipulator which can directly show the reliability of a manipulator through its configuration parameters and identify which component of the manipulator is most critical to its reliability.
3. Plan an experiment to show whether the tested service life is close to the designed or evaluated one or not.

References

[1] Luca Bruzzone and Giorgio Bozzini. “A statically balanced SCARA-like industrial manipulator with high energetic efficiency”. Meccanica 2010; DOI 10.1007/s11012-010-9336-6.

[2] D. A. Streit and E. Shin. “Equilibrators for planar linkages”. ASME Journal of Mechanical Design; 1993; 115: pp. 604-611.

[3] Tsuneo Yoshikawa, Hiroki Murakami, and Koh Hosoda. “Modeling and control a three degree of freedom manipulator with two flexible links”. Experimental Robotics II; 1993; 190: pp. 531-545.

[4] T. Rahman, R. Ramanathan, R. Seliktar, and W. Harwin. “A simple technique to passively gravity-balance articulated mechanisms”. ASME Journal of Mechanical Design; 1995; 117: pp. 655-658.

[5] Clément M. Gosselin and Jiegao Wang. “On the design of gravity-compensated six-degree-of-freedom parallel mechanisms”. In: Proceedings of the 1998 IEEE international conference on robotics and automation; 1998. pp. 2287-84.

[6] A. Gokce and S. K. Agrawal. “Mass center of planar mechanisms using auxiliary parallelograms”. ASME Journal of Mechanical Design; 1999; 121: pp. 166-168.

[7] Jaydeep Roy and Louis L. Whitcomb. “Comparative structure analysis of 2-DOF semi-direct drive linkages for robot arms”. IEEE/ASME Transactions on Mechatronics; 1999; 4(1): pp. 82-86.

[8] Thierry Laliberté, Clément M. Gosselin, and Martin Jean. “Static balancing of 3-DOF planar parallel mechanisms parallel mechanisms”. IEEE/ASME Transactions on Mechatronics; 1999; 4(4): pp. 363-377.

[9] Ion Simionescu and Liviu Ciupitu. “The static balancing of the industrial robot arms, Part I: Discrete balancing”. Mechanism and Machine Theory; 2000; 35: pp. 1287-1298.

[10]Ion Simionescu and Liviu Ciupitu. “The static balancing of the industrial robot arms, Part II: Continuous balancing”. Mechanism and Machine Theory; 2000; 35: pp. 1299-1311.

[11]Kazuo Kobayashi. “Comparison between spring balancer and gravity balancer in inertia force and performance”. ASME Journal of Mechanical Design; 2001; 123: pp. 549-555.

[12]Lionel Birglen and Clément M. Gosselin. “Kinetostatic analysis of underactuated fingers”. IEEE Transactions on Robotics and Automation; 2004; 20(2): pp. 211-221.

[13]Sunil K. Agrawal and Abbas Fattah. “Gravity-balancing of spatial robotic manipulators”. Mechanism and Machine Theory; 2004; 39: pp. 1331-1344.

[14]Abhishek Agrawal and Sunil K. Agrawal. “Design of gravity balancing leg orthosis using non-zero free length springs”. Mechanism and Machine Theory; 2005; 40: pp. 693-709.

[15]Clément M. Gosselin. “Adaptive robotic mechanical systems - a design paradigm”. ASME Journal of Mechanical Design; 2006; 128: pp. 192-198.

[16]Abbas Fattah and Sunil K. Agrawal. “Gravity-balancing of classes of industrial robots”. In: Proceedings of the 2006 IEEE international conference on robotics and automation; 2006. pp. 2872-2877.

[17]Samad A. Hayati. “Assessment of motion of a swing leg and gait rehabilitation with a gravity balancing exoskeleton”. IEEE Transactions on Neural Systems and Rehabilitation Engineering; 2007; 15(3): pp. 410-420.

[18]Clément M Gosselin. “Gravity compensation, static balancing and dynamic balancing of parallel mechanisms”, Smart Devices and Machines for Advanced Manufacturing; 2008: pp. 27-48.

[19]V. Arakelian and S. Ghazaryan. “Improvement of balancing accuracy of robotic systems: application to leg orthosis for rehabilitation devices”. Mechanism and Machine Theory; 2008; 43: pp. 565-575.

[20]Po-Yang Lin, Win-Bin Shieh, and Dar-Zen Chen. “Design of perfectly statically balanced 1-DOF planar linkages with revolute joints only”. ASME Journal of Mechanical Design; 2009; 131: 051004: pp. 1-9.

[21]Sangamesh R. Deepak and G. K. Ananthasuresh. “Static balancing of spring-loaded planar revolute-joint linkages without auxiliary links”. In: Proceedings of the 14th national conference on machines and mechanisms; 2009. pp. 37-44.

[22]Po-Yang Lin, Win-Bin Shieh, and Dar-Zen Chen. “Design of a gravity-balanced general spatial serial-type manipulator”. ASME Journal of Mechanical Design; 2010; 2: 031003: pp. 1-7.

[23]Wan-Kyun Chung and Hyung Suck Cho. “On the dynamic characteristics of a balanced PUMA-760 robot”. IEEE Transactions on Industrial Electronics; 1988; 35(2): pp. 222-230.

[24]Nathan Ulrich and Vijay Kumar. “Passive mechanical gravity compensation for robot manipulator”, In: Proceedings of the 1991 IEEE international conference on robotics and automation; 1991. pp. 1536-1541.

[25]Keiko Homma and Tatsuo Arai. “Design of an upper limb motion assist system with parallel mechanism”. In: Proceedings of the 1995 IEEE international conference on robotics and automation; 1995. pp. 1302-1307.

[26]Mohammad Jashim Uddin, Yasuo Nasu, Kazuhisa Mitobe, and Kou Yamada. “Application of suspension mechanisms for low powered robot tasks”. International Journal of Industrial Robot; 2000; 27(3): pp. 206-216.

[27]Toshio Morita, Fumiyoshi Kuribara, Yuki Shiozawa, and Shigeki Sugano. “A novel mechanism design for gravity compensation in three dimensional space”. In: Proceedings of the 2003 IEEE/ASME international conference on advanced intelligent mechatronics; 2003. pp. 163-168.

[28]Abbas Fattah, Sunil K. Agrawal, Glenn Catlin ,and John Hamnett. “Design of a passive gravity-balanced assistive device for sit-to-stand tasks”. ASME Journal of Mechanical Design; 2006; 128: pp. 1122-1129.

[29]Sai K. Banala, Sunil K. Agrawal, Abbas Fattah, Vijaya Krishnamoorthy, Wei-Li Hsu, John Scholz, and Katherine Rudolph. “Gravity-balancing leg orthosis and its performance evaluation”. IEEE Transactions on Robotics; 2006; 22(6): pp. 1228-1239.

[30]C. Baradat, V. Arakelian, S. Briot, and S. Guegan. “Design and prototyping of a new balancing mechanism for spatial parallel manipulators”. ASME Journal of Mechanical Design; 2008; 130: 072305: pp. 1-13.

[31]Kenan Koser. “A cam mechanism for gravity balancing”. Mechanics Research Communications; 2009; 36: pp. 524-530.

[32]Maja Kolarski, Miomir Vukobratovic, and Branislav Borovac. “Dynamic analysis of balanced robot mechanisms”. Mechanism and Machine Theory; 1994; 29(3): pp. 427-454.

[33]Pi-Ying Cheng and Kuei-Jen Cheng. “A gravity balance mechanism used to eliminate the body-weight influence on people with lower-limb disabilities”. Technology and Disability; 2011; 23(1): pp. 19-28.

[34]Y. H. Andrew Liou, Paul P. Lin, Richard R. Lindeke, and H. D. Chiang. “Tolerance specification of robot kinematic parameters using an experimental design technique – the Taguchi”. Robotics & Computer-Integrated Manufacturing; 1993; 10(3): pp. 199-207.

[35]Zhongxiu Shi. “Reliability analysis & synthesis of robot manipulators”. In: Proceedings of the 1994 annual symposium on reliability and maintainability; 1994. pp. 201-204.

[36]S. S. Rao and P. K. Bhatti. “Probabilistic approach to manipulator kinematics and dynamics”. Reliability Engineering and System Safety; 2001; 72: pp. 47-58.

[37]B. K. Rout and R. K. Mittal. “Tolerance design of manipulator parameters using design of experiment approach”. Structural and Multidisciplinary Optimization; 2007; 34: pp. 445-462.

[38]Bing Li, Li-Yang Xie, Yu-Lan Wei, Ying Wu, Ming-Yang Zhao, and Shi-Zhe Xu. “Reliability Analysis of Kinematic accuracy of a three degree-of-freedom parallel manipulator”. Advanced Materials Research; 2010; 118-120: pp. 743-747.

[39]Jeong Kim, Woo-Jin Song, and Beom-Soo Kang. “Stochastic approach to kinematic reliability of open-loop mechanism with dimensional tolerance”. Applied Mathematical Modelling; 2010; 34: pp. 1225-1237.

[40]Yoshikawa Tsuneo. “Manipulability of robotic mechanisms”, International Journal of Robotics Research; 1985; 4(2): pp. 3-9.

[41]Timothy J. Graettinger. “The acceleration radius-a global performance measure for robotic manipulators”. IEEE Journal of Robotics and Automation; 1988; 4(1): pp. 60-69

[42] C. Gosselin and J. Angeles. “A global performance index for the kinematic optimization of robotic manipulator”. ASME Journal of Mechanical Design; 1991; 113: pp. 220-226.

[43]Kim-Kap Kim and Yong-San Yoon. “Trajectory planning of redundant robots by maximizing the moving acceleration radius”. Robotica; 1992; 10: pp. 195-203.

[44]Byoung Wook Choi, Jon Hwa Won and Myung Jin Chung. “Evaluation of dexterity measures for a 3-link planar redundant

manipulator using constraint locus". IEEE Transactions on Robotics and Automation; 1995; 11(2): pp. 282-285

[45] Keith L. Doty, Melchiorri Claudio, Eric M. Schwartz and Bonivento Claudio. "Robot manipulability". IEEE Transactions on Robotics and Automation; 1995; 11(3): pp. 462-468.

[46]Chiacchio Pasquale. "A new dynamic manipulability ellipsoid for redundant manipulators". Robotica; 2000; 18: pp. 381-397.

[47] Jozsef Kovecses, Robert G. Fenton and William L. Cleghorn. "Effects of joint dynamics on the dynamic manipulability of geared robot manipulator". Pergamon Mechatronics; 2001; 11: pp. 43-58.

[48]Gravagne Ian A, Walker Ian D. "Manipulability and force ellipsoids for continuum robot manipulators". In: Proceedings of the 2001 IEEE international conference on intelligent robots and systems; 2001. pp. 304-311.

[49]Rosenstein Michael T., Grupen Roderic A.. "Velocity-dependent dynamic manipulability". In: Proceedings of the 2002 IEEE international conference on robotics and automation; 2002. pp. 2424-2429.

[50]Bowling Alan P, Khatib Oussama. "The actuation efficiency – a measure of acceleration capability for non-redundant robotic manipulators". In: Proceedings of the 2003 IEEE international conference on intelligent robots and systems; 2003. pp. 3325-3330.

[51]Alan P. Bowling and Khatib Oussama. "The dynamic capability equations-a new tool for analyzing robotic manipulator performance". IEEE Transactions on Robotics and Automation; 2005; 21 (1): pp. 115-123.

[52]Alan P. Bowling and Kim ChangHwan, "Velocity effects on robotic manipulator dynamic performance", ASME Journal of Mechanical Design; 2006; 128: pp. 1236-1245.

[53] Kuei-Jen Cheng and Pi-Ying Cheng. “The investigation of the maneuverability deterioration based on acceleration radius theory”. Mechatronics; 2009; 19: pp. 1211-1220.

[54]Denavit J. and Hartenberg R. S.. “A kinematic notation for lower-pair mechanisms based on matrices”. ASME Journal of Applied Mechanics; 1955; 22: pp. 215-221.

[55]Hayati Samad A. “Robot arm geometric link parameter estimation”. In: Proceedings of the 22nd IEEE international conference on decision and control; 1983. pp. 1477-1483.

[56]Veitchegger WK, Wu Chi-Haur. “Robot accuracy analysis based on kinematics”. IEEE Journal of Robotics and Automation; 1986; 2(3): pp. 171-179.

[57]Veitchegger WK, Wu Chi-Haur. “Robot calibration and compensation”. IEEE Journal of Robotics and Automation; 1988; 4(6): pp. 643-656.

[58]Caenen JL, Angue JC. “Identification of geometric and non geometric parameters of robots”. In: Proceedings of the 1990 IEEE international conference on robotics and automation; 1990. pp. 1032-1037.

[59]Bruno Siciliano, Lorenzo Sciavicco, Luigi Villani, and Giuseppe Oriolo. Robotics: Modelling, Planning and Control analysis, 2nd ed.. London: Springer; 2009.

[60]Saad Mukras, Nam H. Kim, Nathan A. Mauntler, Tony L. Schmitz,W. Gregory Sawyer. “Analysis of planar multibody systems with revolute joint wear”. Wear; 2010; 268: pp. 643-652.